NAVAL POSTGRADUATE SCHOOL
Monterey, California

THESIS

LOCALIZATION OF WIRELESS COMMUNICATION EMITTERS USING TIME DIFFERENCE OF ARRIVAL (TDOA) METHODS IN NOISY CHANNELS

by

Spiros D. Mantis

June 2001

Thesis Advisor: Ralph D. Hippenstiel
Co-Advisors: David C. Jenn
Tri T. Ha

Approved for public release; distribution is unlimited

Form SF298 Citation Data

Report Date *("DD MON YYYY")* 15 Jun 2001	**Report Type** N/A	**Dates Covered (from... to)** *("DD MON YYYY")*

Title and Subtitle LOCALIZATION OF WIRELESS COMMUNICATION EMITTERS USING TIME DIFFERENCE OF ARRIVAL (TDOA) METHODS IN NOISY CHANNELS	**Contract or Grant Number**
	Program Element Number
Authors	**Project Number**
	Task Number
	Work Unit Number
Performing Organization Name(s) and Address(es) Naval Postgraduate School Monterey, CA 93943-5138	**Performing Organization Number(s)**
Sponsoring/Monitoring Agency Name(s) and Address(es)	**Monitoring Agency Acronym**
	Monitoring Agency Report Number(s)
Distribution/Availability Statement Approved for public release, distribution unlimited	
Supplementary Notes	
Abstract	
Subject Terms	
Document Classification unclassified	**Classification of SF298** unclassified
Classification of Abstract unclassified	**Limitation of Abstract** unlimited
Number of Pages 115	

LOCALIZATION OF WIRELESS COMMUNICATION EMITTERS USING TIME DIFFERENCE OF ARRIVAL (TDOA) METHODS IN NOISY CHANNELS

Spiros, D, Mantis-Lieutenant, Hellenic Navy
B.S., Hellenic Naval Academy, 1991
Master of Science in Electrical Engineering and
Master of Science in Systems Engineering–June 2001
Advisor: Ralph, Hippenstiel, Department of Electrical and Computer Engineering
Co-Advisor: David, C., Jenn, Department of Electrical and Computer Engineering
Co-Advisor: Tri, T., Ha, Department of Electrical and Computer Engineering

The ability to provide position information of wireless emitters comprises a very important communication tool and has extremely valuable applications to military as well as civilian life. GSM is the most popular method of modulation adopted around the world, for mobile telephony. This thesis is focused on the Time Difference Of Arrival (TDOA) estimation, applied to GSM signals, in noisy channels. Improvements in denoising, in conjunction with wavelet processing, are proposed for estimating the TDOA of signals received at two spatially separated sensors. Wavelet denoising based on a modified maximum likelihood method and a higher order moment method is proposed, to improve the performance. A numerical evaluation of the methods, when unequal SNR conditions prevail, is presented. The performance of the proposed denoising methods in a jamming environment is also addressed. Simple excision schemes to improve the performance when jamming is present, are evaluated. Simulation results indicate good performance of the methods and improved estimates relative to the ones obtained using no denoising. Jamming presence degrades the performance but still the extracted estimates are improved.

DoD KEY TECHNOLOGY AREA: Electronics,Electronics Warfare.

KEYWORDS: Global System for Mobile (GSM),Time Difference Of Arrival (TDOA),Wavelet Denoising,Jamming,Emitters Localization.

REPORT DOCUMENTATION PAGE			Form Approved OMB No. 0704-0188
Public reporting burden for this collection of information is estimated to average 1 hour per response, including the time for reviewing instruction, searching existing data sources, gathering and maintaining the data needed, and completing and reviewing the collection of information. Send comments regarding this burden estimate or any other aspect of this collection of information, including suggestions for reducing this burden, to Washington headquarters Services, Directorate for Information Operations and Reports, 1215 Jefferson Davis Highway, Suite 1204, Arlington, VA 22202-4302, and to the Office of Management and Budget, Paperwork Reduction Project (0704-0188) Washington DC 20503.			
1. AGENCY USE ONLY *(Leave blank)*	**2. REPORT DATE** June 2001	**3. REPORT TYPE AND DATES COVERED** Master's Thesis	
4. TITLE AND SUBTITLE: Localization of wireless communication emitters using Time Difference Of Arrival (TDOA) methods in noisy channels			**5. FUNDING NUMBERS**
6. AUTHOR(S)			
7. PERFORMING ORGANIZATION NAME(S) AND ADDRESS(ES) Naval Postgraduate School Monterey, CA 93943-5000			**8. PERFORMING ORGANIZATION REPORT NUMBER**
9. SPONSORING / MONITORING AGENCY NAME(S) AND ADDRESS(ES) N/A			**10. SPONSORING / MONITORING AGENCY REPORT NUMBER**
11. SUPPLEMENTARY NOTES The views expressed in this thesis are those of the author and do not reflect the official policy or position of the Department of Defense or the U.S. Government.			
12a. DISTRIBUTION / AVAILABILITY STATEMENT Approved for public release; distribution is unlimited			**12b. DISTRIBUTION CODE**

13. ABSTRACT *(maximum 200 words)*

The ability to provide position information of wireless emitters comprises a very important communication tool and has extremely valuable applications to military as well as civilian life. GSM is the most popular method of modulation adopted around the world, for mobile telephony. This thesis is focused on the Time Difference Of Arrival (TDOA) estimation, applied to GSM signals, in noisy channels. Improvements in denoising, in conjunction with wavelet processing, are proposed for estimating the TDOA of signals received at two spatially separated sensors. Wavelet denoising based on a modified maximum likelihood method and a higher order moment method is proposed, to improve the performance. A numerical evaluation of the methods, when unequal SNR conditions prevail, is presented. The performance of the proposed denoising methods in a jamming environment is also addressed. Simple excision schemes to improve the performance when jamming is present, are evaluated. Simulation results indicate good performance of the methods and improved estimates relative to the ones obtained using no denoising. Jamming presence degrades the performance but still the extracted estimates are improved.

14. SUBJECT TERMS Global System for Mobile, Time Difference of Arrival, Wavelet Denoising, Jamming, Emitter Localization			**15. NUMBER OF PAGES** 111
			16. PRICE CODE
17. SECURITY CLASSIFICATION OF REPORT Unclassified	**18. SECURITY CLASSIFICATION OF THIS PAGE** Unclassified	**19. SECURITY CLASSIFICATION OF ABSTRACT** Unclassified	**20. LIMITATION OF ABSTRACT** UL

NSN 7540-01-280-5500 Standard Form 298 (Rev. 2-89)
Prescribed by ANSI Std. 239-18

THIS PAGE INTENTIONALLY LEFT BLANK

Approved for public release; distribution is unlimited

LOCALIZATION OF WIRELESS COMMUNICATION EMITTERS USING TIME DIFFERENCE OF ARRIVAL (TDOA) METHODS IN NOISY CHANNELS

Spiros D. Mantis
Lieutenant, Hellenic Navy
B.S., Hellenic Naval Academy, 1991

Submitted in partial fulfillment of the
requirements for the degrees of

MASTER OF SCIENCE IN ELECTRICAL ENGINEERING

MASTER OF SCIENCE IN SYSTEMS ENGINEERING

from the

NAVAL POSTGRADUATE SCHOOL
June 2001

Author: _____
Spiros D. Mantis

Approved by: _____
Ralph D. Hippenstiel, Thesis Advisor

_____
David C. Jenn, Co-Advisor

_____
Tri T. Ha, Co-Advisor

_____
Dan Boger, Chairman
Information Warfare Academic Group

_____
Jeffrey B. Knorr, Chairman
Department of Electrical and Computer Engineering

THIS PAGE INTENTIONALLY LEFT BLANK

ABSTRACT

The ability to provide position information of wireless emitters comprises a very important communication tool and has extremely valuable applications to military as well as civilian life. GSM is the most popular method of modulation adopted around the world, for mobile telephony. This thesis is focused on the Time Difference Of Arrival (TDOA) estimation, applied to GSM signals, in noisy channels. Improvements in denoising, in conjunction with wavelet processing, are proposed for estimating the TDOA of signals received at two spatially separated sensors. Wavelet denoising based on a modified maximum likelihood method and a higher order moment method is proposed, to improve the performance. A numerical evaluation of the methods, when unequal SNR conditions prevail, is presented. The performance of the proposed denoising methods in a jamming environment is also addressed. Simple excision schemes to improve the performance when jamming is present, are evaluated. Simulation results indicate good performance of the methods and improved estimates relative to the ones obtained using no denoising. Jamming presence degrades the performance but still the extracted estimates are improved.

THIS PAGE INTENTIONALLY LEFT BLANK

TABLE OF CONTENTS

LIST OF FIGURES

THIS PAGE INTENTIONALLY LEFT BLANK

LIST OF TABLES

THIS PAGE INTENTIONALLY LEFT BLANK

ACKNOWLEDGMENTS

I would like to express my gratitude to Professor Ralph D. Hippenstiel for his help, patience and the numerous hours of counseling that led to the timely and successful completion of this thesis. To my thesis co-advisors, Professor David C. Jenn and Professor Tri T. Ha, a special thanks for their cooperation and consideration.

Finally I would like to thank my wife, Olympia, for her understanding, patience and moral support she provided me during the course of working and writing this thesis. A special mention goes to the Hellenic Navy for giving me the opportunity to be intellectually challenged at the Naval Postgraduate School.

THIS PAGE INTENTIONALLY LEFT BLANK

EXECUTIVE SUMMARY

Emitter localization comprises an important aspect of communications and is valuable in military and civilian applications. The importance of position information of a wireless emitter can be visualized if we consider the emergency 911-call situation when a mobile phone is used. Also, there are military applications in which it's desirable to localize a non-cooperative electromagnetic source.

The most widely used radio frequency (RF) position localization (PL) technique that appears to be superior to others, is the hyperbolic position localization, also known as the Time Difference Of Arrival (TDOA) technique. The TDOA utilizes cross-correlation techniques to estimate the delay of a propagating signal received at two different receivers. This delay estimation defines a hyperbola of constant range difference from the receivers, which are located at their foci. The intersection of a set of three or more hyperbolas provides the PL estimate of the source.

This thesis is focused on the TDOA estimation, applied to GSM signals, generated with the use of the HP-ADS software, in noisy channels. Improvements in denoising, in conjunction with wavelet processing, are proposed for estimating the TDOA of signals received at two spatially separated sensors. We propose two wavelet based denoising methods: the Modified Approximate Maximum Likelihood (MAML) method and the Modified Fourth Order Moment (MFOM) method.

Wavelet decomposition is applied to the output of both receivers. The wavelet coefficients are weighted, in each subband by appropriate factors, which are based on the

received signal statistics. The weighting aims to enhance the frequency bands where the signal is strong and to attenuate the bands when the noise is dominant. The TDOA estimate is obtained, by extracting the lag at which the maximum of the cross-correlation function of the denoised data occurs.

Several situations are studied, primarily the one when unequal signal-to-noise ratio (SNR) conditions prevail, in the presence of Gaussian noise. The performance of the proposed denoising methods in a jamming environment is also addressed. A frequency modulated (FM) noise serves as jamming waveform in the simulations, where we allow the presence of jamming in one of the two channels. The Mean Squared Error (MSE) of the estimated delay is used as criteria of goodness (i.e., low MSE denotes a small error and thus a good localization).

Simulation results indicate good performance of the denoising methods and improved estimates relative to the ones obtained using no denoising. In particular, the application of the MAML method allows a 70.4 to 91.37 percent improvement in the TDOA estimation, depending on the sampling interval. The respective improvement, applying the MFOM method, ranges from 62 to 79 percent. Jamming degrades the performance but still the extracted estimates are improved. A higher degree of correlation of the signal components reduces the probability of error in TDOA estimation.

In addition, we note that in all cases studied the MAML method outperforms the MFOM method. The MAML method appears to be more robust in presence of Gaussian noise and jamming, while the MFOM method shows an undesirable “sensitivity” at low

SNR levels (i.e., -3 dB or less) and when jamming is present. Finally the limits (lowest SNR values), in each channels are obtained above which denoising is beneficial.

I. INTRODUCTION

A. BACKGROUND

Wireless mobile radio systems have generated many new services in recent years. Cellular communication systems provide data and voice communication services with the convenience of mobility to their users. With the development of new Personal Communication Systems (PCS), it is inevitable to expect an increase in the type of services and in the availability of them.

However, one important service, that current wireless radio systems are unable to offer, is efficient and enhanced 911 emergency services. In June 1996, the Federal Communications Commission (FCC) adopted specific regulations, requiring wireless service providers to implement E-911 services [1]. These rules seek to improve the reliability of wireless 911 services and to provide emergency service personnel with location information that enable them to locate and offer assistance to E-911 callers [2].

In September 1999, the FCC revised its rules to better enable carriers to use handset-based location technologies to meet the 1996 requirements [3]. In particular, FCC established separate accuracy requirements and deployment schedules for network-based and handset-based technologies. In brief the localization standards are:

- Handset-based solutions: 50 meters for 67% of calls and 150 meters for 95% of calls
- Network-based solutions: 100 meters for 67% of calls and 300 meters for 95% of calls,

both starting October 1, 2001.

B. OBJECTIVE

Several different position location (PL) techniques are candidates for a wireless PL system [4]. Radio frequency PL systems dominate the field since they appear to be more advantageous, with regard to low cost, ease of integration and potentially high accuracy. Furthermore, these techniques work with no need of modification in the existing cellular/PCS infrastructure.

The most widely used RF PL technique that appears to be superior to others, is the hyperbolic position localization, also known as the Time Difference Of Arrival (TDOA) technique. TDOA utilizes cross-correlation techniques to estimate the delay of a propagating signal received at two receivers. This delay measurement defines a hyperbola of constant range difference from the receivers, which are located at their foci. The intersection of a set of three or more hyperbolas provides the PL estimate of the source.

In this thesis, we will discuss the TDOA estimation and its application to Global System of Mobile (GSM) signals. We will investigate several methods to improve the TDOA estimate and the performance of these methods when unequal SNR conditions prevail. Furthermore, the sensitivity to jamming will be studied.

C. THESIS OUTLINE

The first chapter gives a general background and an introduction to the problem. Chapter II introduces the GSM system. Chapter III presents the various position localization techniques that are used, with a more detailed discussion of the TDOA and the extraction of its estimate. Chapter IV examines the wavelet based denoising methods,

to improve TDOA estimation. Chapter V discusses the GSM test signals and the jamming waveform generation used in the simulations. Chapter VI presents the unequal SNR and the jamming simulation results. Finally, Chapter VII contains the conclusions as well as suggestions for future work on this topic.

THIS PAGE INTENTIONALLY LEFT BLANK

II. GLOBAL SYSTEM FOR MOBILE (GSM)

A. GSM HISTORY

The Global System for Mobile communications is a digital cellular communications system. It was developed in order to create a common European mobile telephone standard but it has been rapidly accepted worldwide.

In 1982 the Conference of European Posts and Telecommunications (CEPT) formed a study group to analyze and develop a Pan-European public land mobile system [5]. This system had to meet certain criteria such as

- Support of International roaming
- Low terminal and service cost
- Good speech quality
- Spectral efficiency
- ISDN compatibility (Integrated Services Digital Network)
- Support a variety of new services and facility

In 1989, the European Telecommunication Standards Institute (ETSI) took the responsibility and the phase I GSM specifications were established in 1990 [6]. Commercial use and service was started in 1991 and by 1994 there was a 1.3 million, subscriber population worldwide, which grew to almost 380 million by December 2000.

In 1995 the phase II GSM specifications where completed, which included the adaptation of North America's PCS 1900, which mainly aimed to standardize the coverage of rural areas.

Today more than 200 GSM networks (including PCS 1900) are operational in 110 countries around the world. The GSM Association estimates that by the end of 2001 the

number of subscribers will be around 500 million, and by the end of 2004, this number will increase to 730 million worldwide [6].

B. GSM RADIO SYSTEM

GSM utilizes two bands of 25 MHz, one for the forward link (base station to mobile) at 935-960 MHz and the 890-915 MHz for the reverse link (mobile to base stations). The combined use of Time Division Multiple Access (TDMA) and Frequency Division Multiple Access (FDMA) schemes, provide the ability of simultaneous access for multiple users.

The available bandwidth of 25 MHz is divided among 124 channels of 200 KHz each. It should be noted that there are 125 channels. One is not used on purpose to prevent interference from other neighboring non-GSM systems. This channel is divided into a 100 KHz guard band at the upper and the lower end of the GSM spectrum. Different carrier frequencies are used for each of the 124 channels. Each individual channel is time division multiple accessed by users at different locations within a cell site. Time is segmented into intervals called frames. Each frame is further partitioned into assignable, non-overlapping, user time slots. The frame duration is 4.615 milliseconds and is divided among eight timeslots, each of which is occupied by an individual user. Radio transmissions on both the forward and the reverse link are made at a channel data rate of 270.833 Kbps, using binary Gaussian Minimum Shift Keying (GMSK) modulation with a 3dB bandwidth-bit-period product (BT) of 0.3.

This data rate implies a bit duration of 3.7 μsec and an effective channel transmission rate per user, of 33.854 Kbps (270.833 Kbps/8 users).

The total number of available channels within the 25 MHz band is 1000 (125 x 8). The GSM frame structure is presented in Figure 2.1 [7].

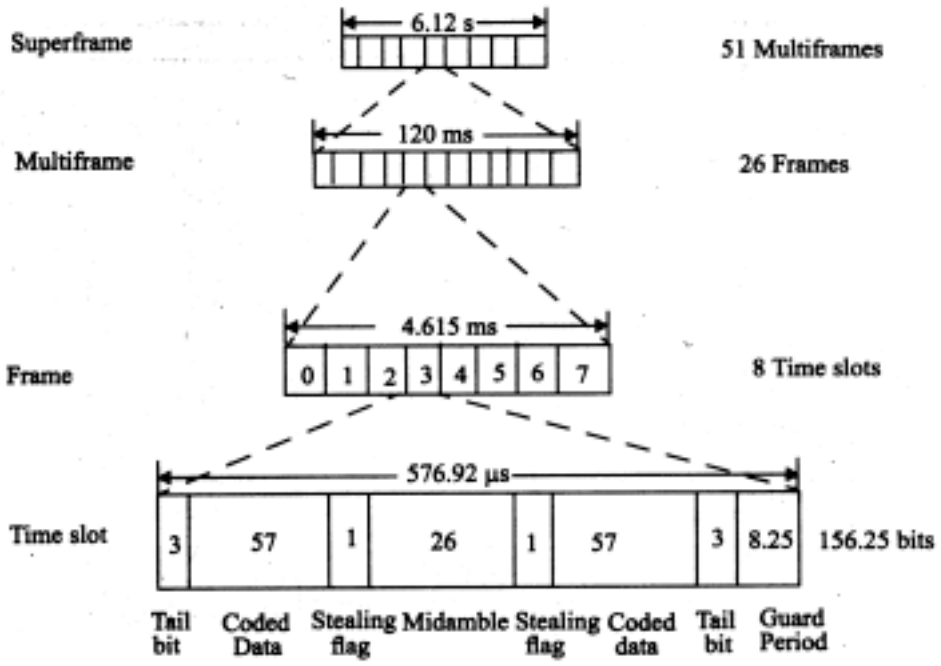

Figure 2.1. GSM Frame Structure "From Ref. [7]."

It is also worth mentioning that there are higher order frames, called multi-frames, within the GSM structure. The highest order frame is called a hyper-frame and has a time duration of 3 hours 28 minutes and 52.76 seconds. This long period of a hyper-frame is required to support encryption with high security. The extended and detailed

description of the higher order frames are out of the scope of this thesis and the reader can find the details in [7, 8].

C. GMSK MODULATION

The Gaussian Minimum Shift Keying (GMSK) is a binary modulation scheme, which can be viewed as a derivative of the Minimum Shift Keying (MSK). In GMSK, applying a baseband Gaussian-shaped filtering to the Non-Return-to-Zero (NRZ) modulated data prior to modulation reduces both the side lobe power level and the width of the main lobe. Figure 2.2 illustrates a simple block diagram of a GMSK modulator.

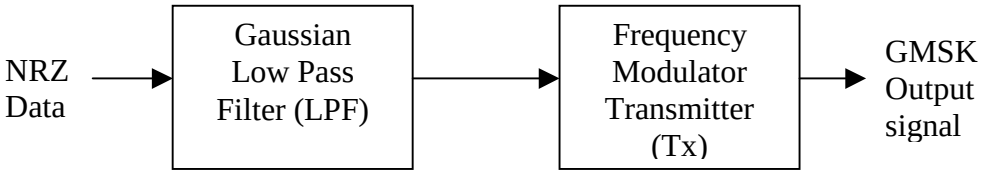

Figure 2.2. Simple GMSK Modulator

The use of the pre-modulation Gaussian filtering smoothes the phase trajectory and hence stabilizes the instantaneous frequency variations over time, which leads to the reduction of the side lobe power spectral levels [8]. However, intersymbol interference (ISI) is introduced, because filtering converts the full response message signal into a partial response scheme where each transmitted symbol spans several bit periods T [9]. This is evident if we examine Figure 2.3, which depicts the impulse response of a Gaussian filter for a BT product of 0.3 and 0.5.

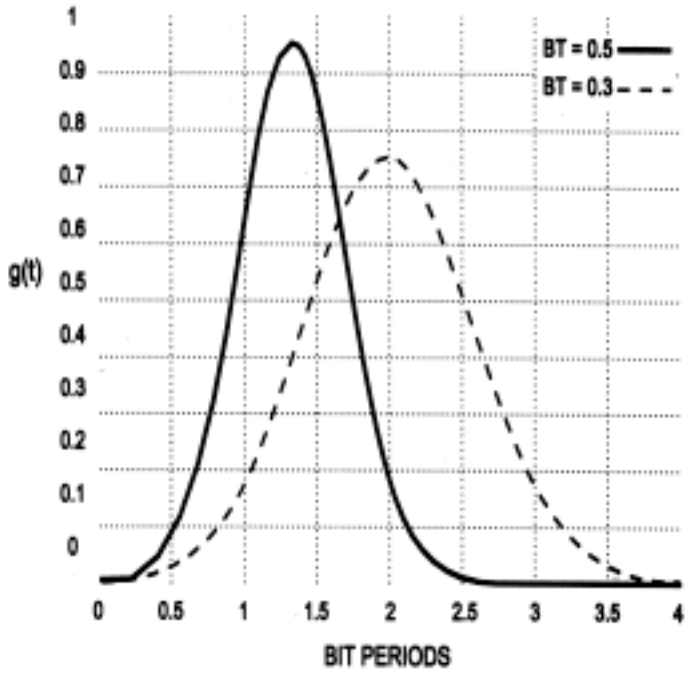

Figure 2.3. Gaussian Filter Impulse Response for BT = 0.3 and BT = 0.5

Referring to Figure 2.3, we notice that a bit is spread over approximately 3 bit periods for BT = 0.3 and two bit periods for BT= 0.5. This is the reason that ISI phenomena arise with the use of the pre-modulation Gaussian filter. It is clear that as the product BT decreases, the ISI increases.

A plot of the spurious radiated power in the adjacent channel to the desired channel power, with normalized frequency separation $(f-f_s)T$ (for GSM is $200 \cdot 10^3 \frac{2}{270.833 \cdot 10^3} \cong 1.5$) on the abscissa and the 3dB bandwidth–bit-duration product BT of the pre-modulation Gaussian filter, as parameter, is shown in Figure 2.4 [8].

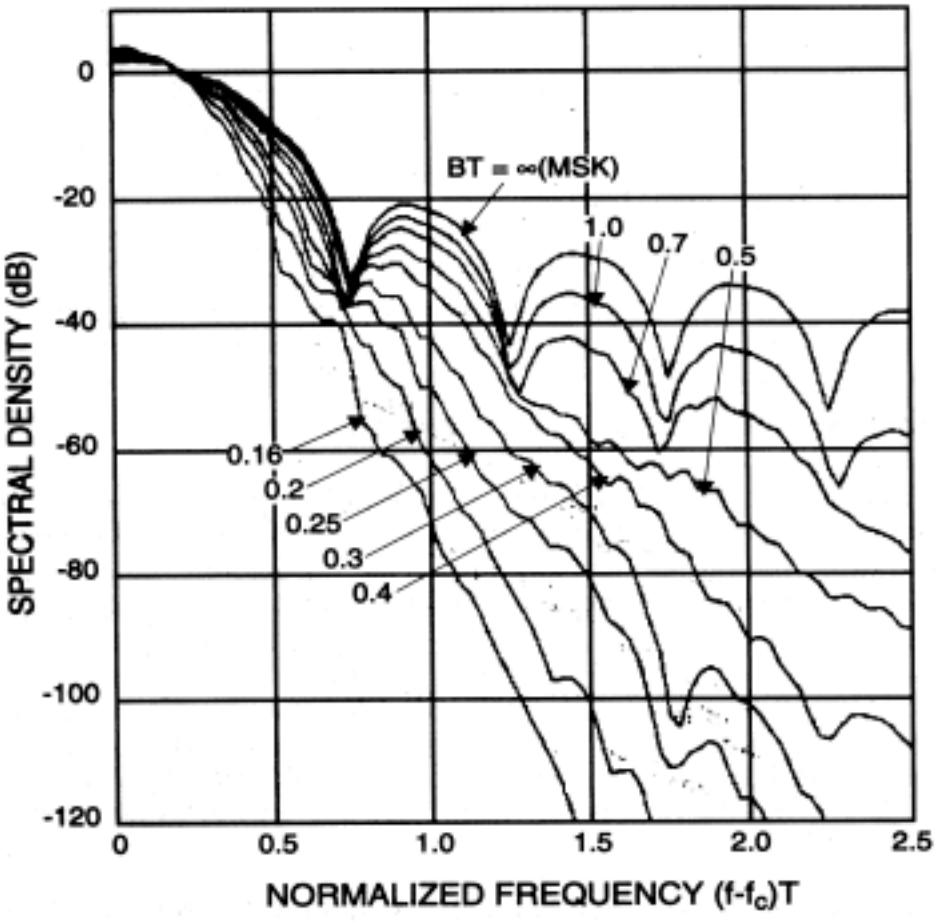

Figure 2.4. Power Spectral Density of GMSK (BT as parameter) "From Ref. [8]"

We can see that while the GMSK spectrum becomes more compact (Figure 2.4) as the BT decreases, the degradation due to ISI increases (Figure 2.3). GMSK sacrifices the irreducible error rate, due to ISI, for very good spectral efficiency due to the constant envelope properties.

For the GSM systems, GMSK with a BT of 0.3 at a channel data rate of 270.8 Kbps has been adopted, since it appears to be an optimum compromise between bit error

rate and out-of-band interference. The value 0.3 represents the 3 dB bandwidth-bit-duration product or normalized pre-Gaussian bandwidth, which corresponds to a filter bandwidth of 81.25 KHz for a bit rate of 270.833 Kbps.

THIS PAGE INTENTIONALLY LEFT BLANK

III. POSITION LOCATION TECHNIQUES

A. TECHNIQUES

It is inevitable that wireless communication carriers must have the ability to provide localization of every mobile device. This inevitability is validated by the Federal Communications Commission (FCC) requirement for the wireless emergency 911 services [1, 2, 3, and 4], in the United States.

In order to comply with the FCC ruling the carrier must provide positioning solutions that do not require the users to take any action in order to be located. There are three basic approaches to obtain position information that do not require modification of the mobile units, which are briefly described below.

1. Angle of Arrival (AOA)

The Angle of Arrival method utilizes multi-array antennas at cell site locations and tries to estimate the direction of arrival of the signal of interest. This implies that a single AOA measurement restricts the source location along the line in our estimated direction. In general multiple AOA estimates are needed to improve the unit's location estimate, which is based on the point of intersection of the projected lines drawn out from the cell site at the angle from which the signal originated.

Algorithms that exploit the phase differences between closely spaced antenna elements of an antenna-array provide the estimate of AOA. The spacing between the elements of the array is typically less than ½ wavelength of the received signal. This is required to avoid ambiguity in the estimating of the arrival angles. The resolution of

AOA estimates improves as the distance between the elements increases, however this improvement is at the expense of introducing ambiguities.

Although angle of arrival has been well developed among military and government organizations, since it requires no special modifications to mobile devices, there are certain drawbacks.

One important issue is that AOA is extremely sensitive to wide-angle reflections (multi-path) that occur when a device is operating in heavily shadowed channels, such as those encountered in urban environments. These reflections may provide power levels stronger than the Line-of-Sight (LOS) direction, thus an incorrect calculation of angle. However, the application of a technique known as Correlation Interferometry Direction Finding (CIDF) [10] provides efficient solution to the problem. This technique employs cross-correlation and uses a calibration database to determine AOA. The technique provides automatic compensation for the errors that the multi-path may introduce. The effectiveness of this method is evident from the fact that it has been successfully applied to shipboard High Frequency Direction Finding (HFDF) system, as discussed in Reference [11].

Another factor is the considerable cost of installation of antenna arrays, although the future use of “smart antennas” [12], which are compact arrays that shape the cell site transmitter and receiver signals into a beam that focuses on the mobile unit, is very promising.

Finally the accuracy of the AOA estimate is reduced as the mobile unit moves away from a cell site or moves from cell to cell and the call is handed off from channel to channel.

2. Time Of Arrival (TOA)

Time of arrival is another well-known technique used to determine the location of mobile units. The key point in this method is to determine the time it takes, for the signal, to travel from the source to the receiver on the forward or the reverse link. For this purpose, the base station transmits an inquiry to the mobile unit and measures the time in which the unit responds. The total measured time corresponds to the round trip signal delay plus the processing delay of the mobile unit.

If the processing delay is known with sufficient accuracy then the round trip delay can be determined. Thus, using this time measurement, the distance between the unit and the receiver can be estimated. Taking the estimated distances from other two base stations, the position of the mobile is extracted by triangulation.

It is obvious that timing errors in the absence of Line-of-Sight (LOS) are significant and very important in the estimation of the unit's location. The impact of the multi-path reflections appears to be very strong, decreasing the accuracy of the estimated position. In practice it might be difficult for the base stations to estimate the response delay of the mobile unit with sufficient accuracy.

3. Time Difference Of Arrival (TDOA)

This method is well suited to estimate the location of wireless devices, since it is applicable with both brief transmissions, such as the reverse control channel, and with longer transmissions, such as the reverse voice channel [13]. This technique is based, in principal, on estimating the difference of arrival times of a signal received at multiple receivers.

The most common approach to obtain TDOA estimates, applies cross-correlation between the signals arriving at two spatially separated base stations. The lag that maximizes the cross-correlation functions represents the TDOA estimate.

In addition, the cross-correlation is used to determine at which base station the signal arrived first. The combination of the estimates of two or more pairs of base stations yields hyperbolic curves along which the mobile may lie. The intersection of these curves provides the position estimate.

We have to point out that it is essential, for the accuracy of this technique, that all of the base stations have a synchronized time reference. This means that a precise timing of a mobile's signal transmission must be maintained at various cell sites. This is accomplished by using a common time base at the base stations.

This technique offers many positive benefits as compared to other position localization techniques. Although both AOA and TDOA techniques rely mainly on a direct LOS between mobile and base stations, multi-path components affect TDOA less [13]. This is true in situations where the multi-path reflections affect all the stations involved in the localization process. The timing errors introduced may be cancelled or reduced in the time difference process [14]. Additionally TDOA does not require knowledge of the absolute time of transmission from the unit, which in general is more difficult to determine. Lower implementation cost is also an advantage since TDOA techniques can be used with the existing equipment and simple, inexpensive conventional antennas (i.e., whip antennas).

B. TDOA ESTIMATION AND POSITION LOCALIZATION

The position localization process consists of two distinct parts. One is the computation of accurate TDOA estimates. This process in general involves denoising techniques that aim to discard the undesirable presence of noise in the signal of interest. The most popular denoising techniques are based on wavelet decomposition and will be presented in detail in the next chapter.

The second part of the process uses the TDOA estimates to extract the position of the unit. We will briefly discuss both processing stages and point out the principle idea behind each one.

1. Determination Of TDOA Estimates

The most popular method to obtain TDOA estimates is the generalized cross-correlation method. The transmitted signal *s(t)*, when it is received by the base stations will be delayed and corrupted by noise and can be represented as follows

$$x(t) = \alpha\, s(t - d_x) + n_x(t) \qquad (3.1)$$

$$y(t) = \beta\, s(t - d_y) + n_y(t) \qquad (3.2)$$

where d_x, d_y are the time delay from the transmitter unit to receiver *x* and *y* respectively and, α, β are coefficients such that $0 < \alpha, \beta \leq 1$.

Bearing in mind that the receiving base stations are synchronized, so that a common time base is established, the cross-correlation function of the received signal is computed as [13]

$$\hat{R}_{xy}(\tau) = \frac{1}{T} \int_0^T x(t)\, y(t+\tau)\, dt \qquad (3.3)$$

Once $\hat{R}_{xy}(\tau)$ is computed, the lag that maximizes (3.3) is considered to be the estimate for the TDOA value.

2. Determination Of Position Estimate

When the previous process is completed, the TDOA estimates are available. Each estimate localizes the unit on a hyperboloid with a constant range difference between the two base stations. This range difference is given by

$$R_{i,j} = \sqrt{(X_i - x)^2 + (Y_i - y)^2 + (Z_i - z)^2} - \sqrt{(X_j - x)^2 + (Y_j - y)^2 + (Z_j - z)^2} \qquad (3.4)$$

where (X_i, Y_i, Z_i) and (X_j, Y_j, Z_j) represent the coordinates of the base stations *i* and *j* and *(x, y, z)* are the possible mobile unit coordinates [13]. Of course, the mobile unit only occupies one point on the hyperbolic curve.

Using three pairs of base stations and substituting the TDOA estimates in equation (3.4), we can estimate the location of the mobile unit. Several methods are available for solving the hyperboloid equations with great accuracy and a detailed presentation can be found in References [15, 16, 17].

IV. DENOSING METHODS TO IMPROVE TDOA ESTIMATE

In this chapter we will present the details of the denoising methods, used to improve the accuracy of the TDOA estimate. This is a crucial issue, that directly influences the position localization estimate of a mobile unit, as pointed out in section III.B.2.

Generally speaking, the denoising process consists of three phases: (a) wavelet transform of the received signal, (b) thresholding of the decomposition coefficients and (c) inverse wavelet transform of the modified coefficients.

A signal emanating from a remote source, embedded in noise and sampled at two spatially separated sensors can be modeled as

$$x(k) = s(k) + n_x(k) \tag{4.1}$$

$$y(k) = s(k+d) + n_y(k) \quad k = 0,1,2,\ldots,N-1 \tag{4.2}$$

where *s(k)* is the unknown signal, which is assumed to be independent of the noise and α and β coefficients are set to one. The components $n_x(k)$ and $n_y(k)$ are additive uncorrelated Gaussian noise sequences that control the signal-to-noise ratio (SNR). The quantity *d* is the time difference of arrival and *N* is the number of samples collected at each receiver.

The methods proposed to increase the accuracy of the TDOA estimation are generically depicted in Figure 4.1. The noise at each receiver is effectively reduced, by using wavelet based denoising on both channels.

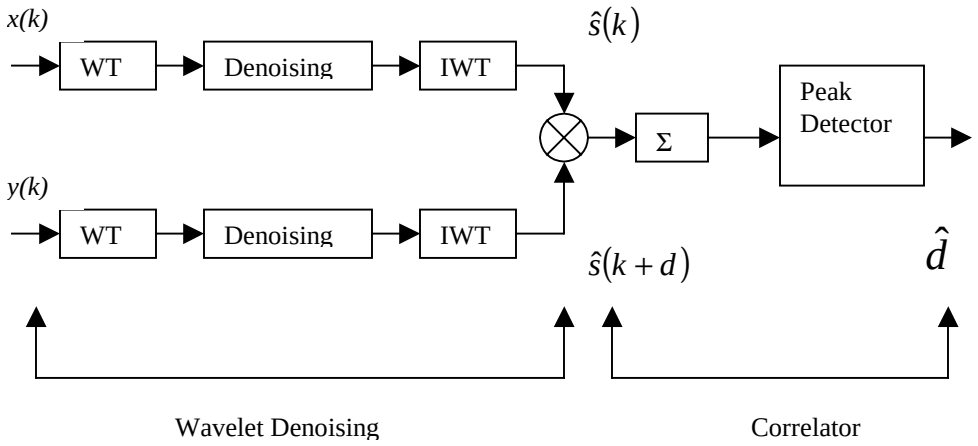

Figure 4.1. Block diagram for TDOA estimation using wavelet denoising

A. MODIFIED APPROXIMATE MAXIMUM LIKELIHOOD (MAML) METHOD

The Approximate Maximum Likelihood (AML) method was proposed by Y.T. Chan, H.C. So, and P.C. Ching for estimation of the TDOA of signals [18]. It aims to attenuate the noise in the subbands where the noise is strong and to enhance the signal at the subbands where it is strong, by appropriate weighting of the decomposition coefficients. The prefilters $H_x(f)$ and $H_y(f)$, shown in Figure 4.2, are chosen to satisfy [18]

$$H_x(f)H_y^*(f) = \frac{\dfrac{G_{ss}(f)}{G_{n_x n_x}(f)G_{n_y n_y}(f)}}{1+\dfrac{G_{ss}(f)}{G_{n_x n_x}(f)}+\dfrac{G_{ss}(f)}{G_{n_y n_y}(f)}} \qquad (4.3)$$

where $G_{ss}(f)$, $Gn_xn_x(f)$, and $Gn_yn_y(f)$ denote the auto-power spectra of $s(k)$, $n_x(k)$, and $n_y(k)$, respectively. This choice of the pre-filters is known as maximum likelihood (ML) weighting.

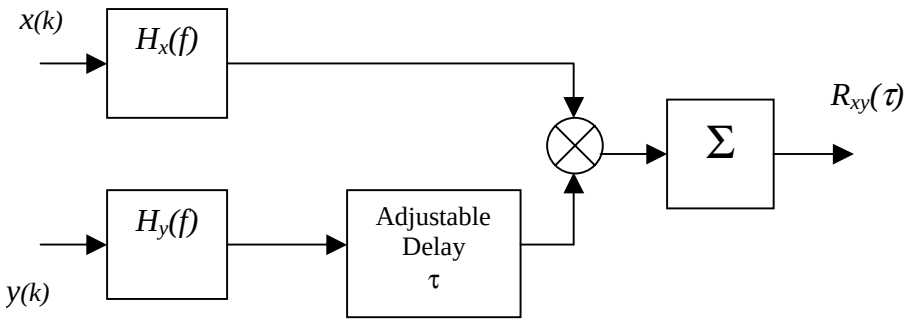

Figure 4.2. Generalized cross-correlator

The AML filtering is performed by weighting the noisy signal in each decomposition level. The weights are determined level by level, so that a large delay variance is avoided. The derivation of these weights assumes that the signal component in each subband can be approximated by a flat spectrum. This assumption leads to the idea that the optimal weighting function and the auto-power spectrum of the signal, are modeled by a piecewise constant functions. This makes sense, particularly when the number of the decomposition levels is sufficiently large.

Using the above, the weights for the detail coefficients are given by

$$w_{d_i} = \frac{\hat{\sigma}^2_{sd_i}}{\hat{\sigma}^2_{n_1 d_i}\hat{\sigma}^2_{n_2 d_i} + \hat{\sigma}^2_{sd_i}\left(\hat{\sigma}^2_{n_1 d_i} + \hat{\sigma}^2_{n_2 d_i}\right)} \qquad (4.4)$$

where, *i=1,2,…J*, and *J* is the number of the wavelet decomposition levels, [18].

Under the assumption that the wavelet filter's gain is two and the filter transfer function is ideal, the noise power will remain the same after passing through each filter. The estimates for the noise and the signal powers are computed as follows:

$$\hat{\sigma}_s^2 = \arg\max \hat{R}_{xy}(\tau) \tag{4.5}$$

$$\hat{\sigma}^2_{\mathrm{n}_1 d_i} = \hat{\sigma}^2_{n_1} = \frac{1}{N}\sum_{k=0}^{N-1}(x(k))^2 - \hat{\sigma}_s^2 \tag{4.6}$$

$$\hat{\sigma}^2_{\mathrm{n}_2 d_i} = \hat{\sigma}^2_{n_2} = \frac{1}{N}\sum_{k=0}^{N-1}(y(k))^2 - \hat{\sigma}_s^2 \tag{4.7}$$

$$\hat{\sigma}^2_{sd_i} = \frac{1}{T_i}\sum_{k=0}^{T_i-1}\left(d_i(k)\right)^2 - \hat{\sigma}^2_{n_1} \tag{4.8}$$

The quantity $\hat{\sigma}_s^2$ denotes the estimate of the total input signal power, $\hat{\sigma}^2_{n_1}$ and $\hat{\sigma}^2_{n_2}$ represent the estimated noise powers, and $\hat{\sigma}^2_{sd_i}$ is the estimated signal power in the subband "*i*". The quantities *N* and T_i represent the number of elements of the signal sequence and the number of elements in each subband, respectively. A modified weight, compared to the one proposed in [19], is used for the last approximate coefficient of the wavelet decomposition, as follows:

$$w_{a_J} = \frac{\hat{\sigma}^2_{sa_J}}{\hat{\sigma}^2_{n_1}\hat{\sigma}^2_{n_2} + \hat{\sigma}^2_{sa_J}\left(\hat{\sigma}^2_{n_1} + \hat{\sigma}^2_{n_2}\right)} \tag{4.9}$$

where

$$\hat{\sigma}^2_{sa_J} = 2^J \hat{\sigma}^2_s - \sum_{i=1}^{J} 2^{J-i} \hat{\sigma}^2_{sd_i} \tag{4.10}$$

The $\hat{\sigma}^2_{sa_j}$ is the estimated signal power in the approximate coefficient of the wavelet decomposition at level *J*. The modified coefficients are obtained as:

$$d_{i_{\text{mod}}} = w_{d_i} \cdot d_i \qquad i = 1, 2, \ldots J \tag{4.11}$$

After weighting each decomposition coefficient, the inverse wavelet transform is used to reconstruct the denoised signal, from the modified coefficients. The adaptation of the AML method and its application in both channels is referred to as the Modified Approximate Maximum Likelihood (MAML) method.

One important issue is to determine the number of the appropriate decomposition levels, in order to avoid considerable variances in the power estimates (especially when the number of elements in the decomposition coefficient is small). A simple assumption is made to avoid large variances. If the adjacent subband signal power is small then we interrupt the decomposition. By trial and error, for the GSM signal that we are using, we found that if the ratio of the power of the approximate coefficient, to the power of the detail coefficient, in a given scale (level), is smaller that 0.5, we can terminate the decomposition procedure without a measurable loss.

B. MODIFIED FOURTH ORDER MOMENT (MFOM) METHOD

1. Background

White Gaussian noise has samples that are statistically independent. If *z* is a random vector of *N* consecutive samples from a real valued, zero mean, white Gaussian process, its probability function is given by [20]:

$$f(z_0, z_1, \ldots, z_{N-1}) = \prod_{n=0}^{N-1} \frac{1}{\sqrt{2\pi\sigma_0^2}} \cdot e^{\frac{(z_n)^2}{2\sigma_0^2}} \tag{4.12}$$

The moments of a stationary process are given by [20]

$$M_z^{(1)} = E\{z[n]\} = m_z \tag{4.13}$$

$$M_z^{(2)}[l_1] = E\{z[n]z[n+l_1]\} = R_z[l_1] \tag{4.14}$$

$$M_z^{(3)}[l_1, l_2] = E\{z[n]z[n+l_1]z[n+l_2]\} \tag{4.15}$$

$$\begin{aligned} M_z^{(4)}[l_1, l_2, l_3] &= E\{z[n]z[n+l_1]z[n+l_2]z[n+l_3]\} \\ &= E\{z[n]z[n+l_1]\}E\{z[n+l_2]z[n+l_3]\} \\ &+ E\{z[n]z[n+l_2]\}E\{z[n+l_1]z[n+l_3]\} \\ &+ E\{z[n]z[n+l_3]\}E\{z[n+l_1]z[n+l_2]\} \end{aligned} \tag{4.16}$$

and

$$M_z^{(4)}[0,0,0] = 3 \cdot \sigma_z^4 \tag{4.17}$$

The fourth order moment of the received signal, i.e. $x(k)=s(k)+n_1(k)$, is computed as follows:

$$
\begin{aligned}
M_x^{(4)}[0,0,0] &= E\left\{\left(s(k)+n_1(k)\right)^4\right\} \\
&= E\left\{s^4[k]\right\}+4E\left\{s^3[k]n_1[k]\right\}+6E\left\{s^2[k]n_1^2[k]\right\} \\
&+4E\left\{s[k]n_1^3[k]\right\}+E\left\{n_1^4[k]\right\} \\
&\geq 3\sigma_{n_1}^4
\end{aligned} \tag{4.18}
$$

Going a little bit further, one can compute the mean and the standard derivation of the fourth order moment. If we define $p = M_z^{(4)}$, then the mean of *p* is:

$$E\{p\} = \frac{1}{N}\sum_{i=0}^{N-1} E\left\{z_i^4\right\} = 3\sigma_z^4 \tag{4.19}$$

In addition, the second moment and the variance are:

$$E\left\{p^2\right\} = \frac{\sigma_z^8}{N}(9N+96) \tag{4.20}$$

$$\sigma_p^2 = \frac{96}{N}\sigma_z^8 \tag{4.21}$$

2. Method

In the proposed method we accounted for the variability of the estimate by choosing a threshold of $3.1\hat{\sigma}_{n_1}^4$, equation (4.19).

It is evident that the fourth order moment of the detail decomposition coefficient, which contains signal, will be greater than $3\hat{\sigma}_{nd_i}^2$, where $\hat{\sigma}_{nd_i}^2$ is computed in equations (4.6) and (4.7) and "*i*" denotes the decomposition level. This fact is used to eliminate the wavelet coefficients in which the noise is dominant and keep the ones where the signal is strong. The estimates of the signal and noise powers are computed according to equations (4.5), (4.6), and (4.7).

The noise power, after passing through the first high pass filter is

$$\hat{\sigma}^2_{n_j d_1} = \frac{G \cdot \hat{\sigma}^2_{n_j}}{2} \qquad j = 1,2 \qquad (4.22)$$

where G is the gain of the high and low pass filters, at decomposition level 1.

Assuming that the filter gain is 2, then the noise power of any detail decomposition coefficient d_i is

$$\hat{\sigma}^2_{n_j d_i} = \frac{G^i \cdot \hat{\sigma}^2_{n_j}}{2^i} = \hat{\sigma}^2_{n_j} \qquad j = 1,2 \qquad (4.23)$$

We modify each wavelet decomposition coefficient as follows:

$$d_{i_{\text{mod}}} = \begin{cases} d_i & ; \text{ if } E\{d_i^4\} \geq 3.1 \cdot \hat{\sigma}^4_{n_1} \\ 0 & ; \text{ otherwise} \end{cases} \qquad (4.24)$$

We introduce a modification in the above presented method. Prior to the application of equation (4.24) an additional threshold is used to pre-filter the wavelet decomposition coefficients in time. Based on the previous discussion, the power contained in each element of the decomposition coefficient, which represent signal, will be greater than $\sqrt{3.1\hat{\sigma}^4_{n_1}}$. Thus, the empirical threshold corresponding to the square root of $3.1\hat{\sigma}^4_{n_1}$ is used. This threshold is compared with the squared value of each element of the decomposition coefficients. If the elements have a squared value less than $\sqrt{3.1\hat{\sigma}^4_{n_1}}$ they are set to zero, otherwise they are left unchanged. After modifying the coefficients, the fourth order method described previously is applied. Finally, the resultant modified coefficients are combined to reconstruct the denoised signal using the inverse wavelet

transform. We have to mention that the procedure described in Section IV.A (i.e. minimize the number of decomposition levels) is also applied.

C. COMBINED DENOISING METHODS

In our effort to eliminate the noise in the GSM noisy signal, we try combining denoising schemes, using the previously presented methods. The combined schemes are depicted in the block diagrams of Figure 4.3. Even though the resulting denoised signal is satisfactory, the combined schemes do not outperform the individually applied denoising methods.

The results and the performance of the combined schemes, as compared to the individually applied over, are presented in Appendix [A].

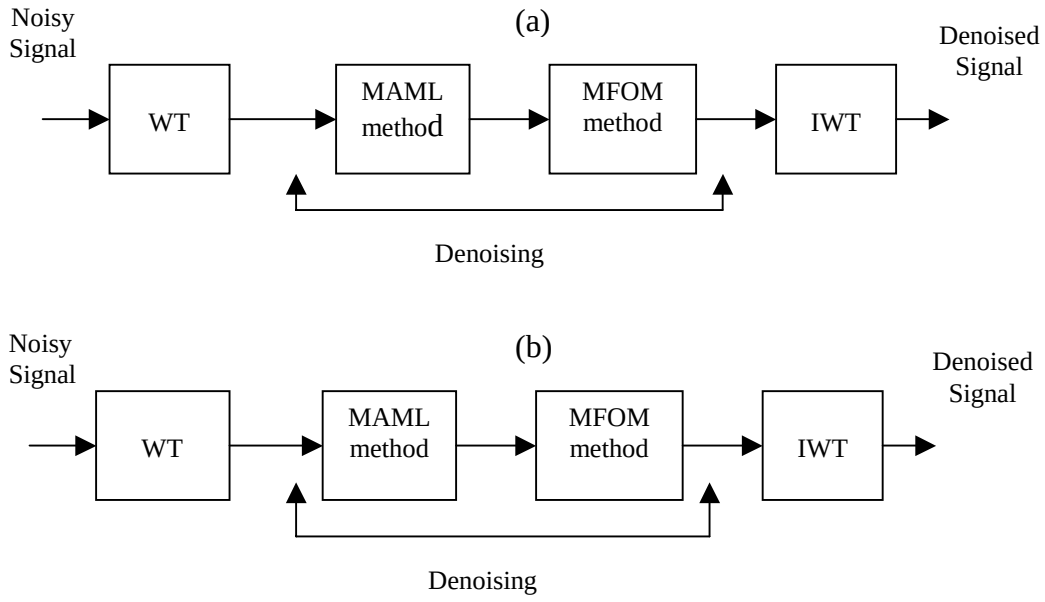

Figure 4.3. Combined denoising schemes

THIS PAGE INTENTIONALLY LEFT BLANK

V. TEST GSM SIGNALS AND JAMMING SIGNAL DESCRIPTIONS

A. GSM SIGNAL

The Hewlett-Packard Advanced Design System (HP-ADS) was used to generate the test GSM signals, for our simulation purposes.

The HP-ADS is a very powerful and reliable tool for engineers [21], since it offers the ability to the user to customize and evaluate many different design aspects of communications, digital signal processing, and a variety of other system parameters. The HP-ADS software provides an excellent method to obtain signal details that are essentially identical to the ones encountered in an actual cellular communication system. Detailed operating instructions of the HP-ADS program and a more specific view of each of its components can be found in Reference [22].

Using the communications package of the HP-ADS, we generate a GSM signal, sampled at three different sampling rates [22]. The specifications of the GSM signal discussed in Chapter II are used as inputs. The specified symbol period of 3.7 microseconds is used. The filter bandwidth at the receiver is 1.2 MHz, which implies that the minimum, non-violating the Nyquist criterion, sampling frequency is 2.4 MHz. The parameters of the test signals are summarized in Table 5.1.

Samples/Symbol	Sampling Interval (nsec)	Sampling Frequency (MHz)	Symbols per 600 samples
40	92.59	10.8	15
20	185.185	5.4	30
10	370.370	2.7	60

Table 5.1. Test GSM signal parameters

The I and Q channel outputs of each test signal, are shown in Figures 5.1, 5.2, and 5.3. It is evident that as the sampling interval increases, so does the variation in the GSM signals.

The reason for this is obvious, if we consider that for a constant number of samples (600), we are using in all simulations, a lower sampling frequency captures more information (symbols) than a higher one.

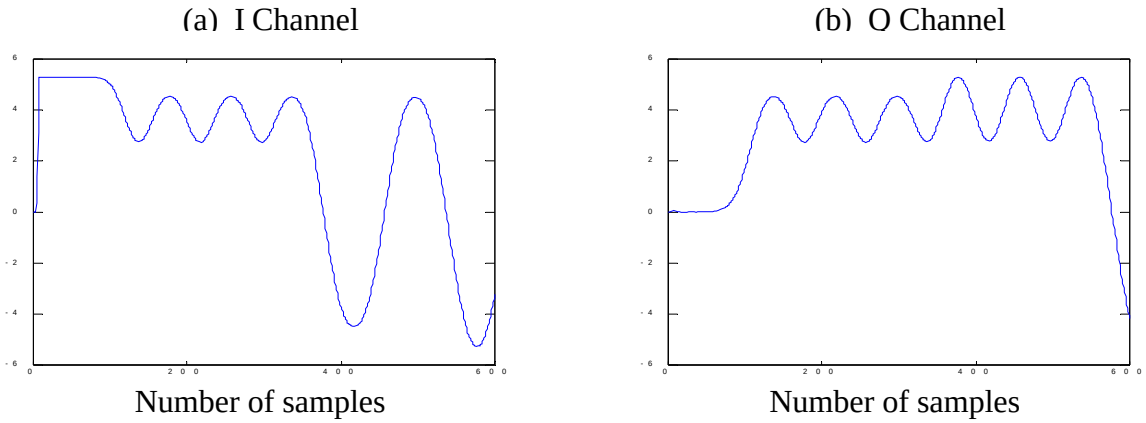

Figure 5.1. I and Q channels of the HP-ADS data with T_s=92.59 (nsec)

(a) I Channel

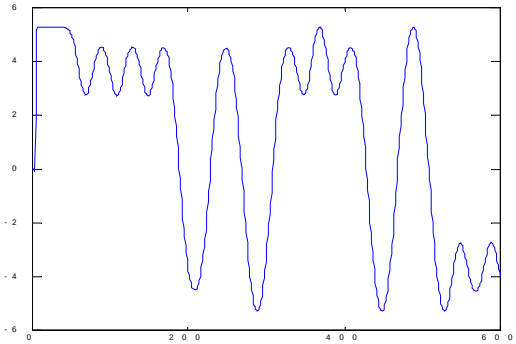

(b) Q Channel

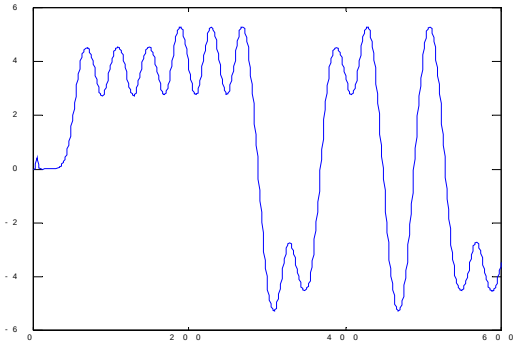

Figure 5.2. I and Q channels of the HP-ADS data with T_s=185.185 (nsec)

(a) I Channel

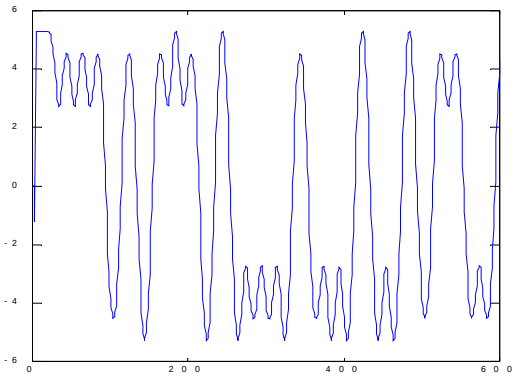

(b) Q Channel

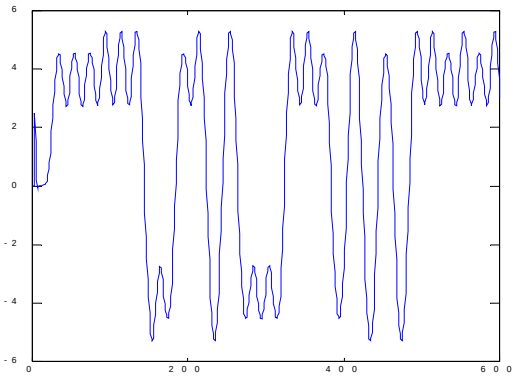

Figure 5.3. I and Q channels of the HP-ADS data with T_s=370.370 (nsec)

At this point, we have to mention the auto-correlation characteristics of this set of samples. The respective auto-correlations of the test signals are shown in Figure 5.4.

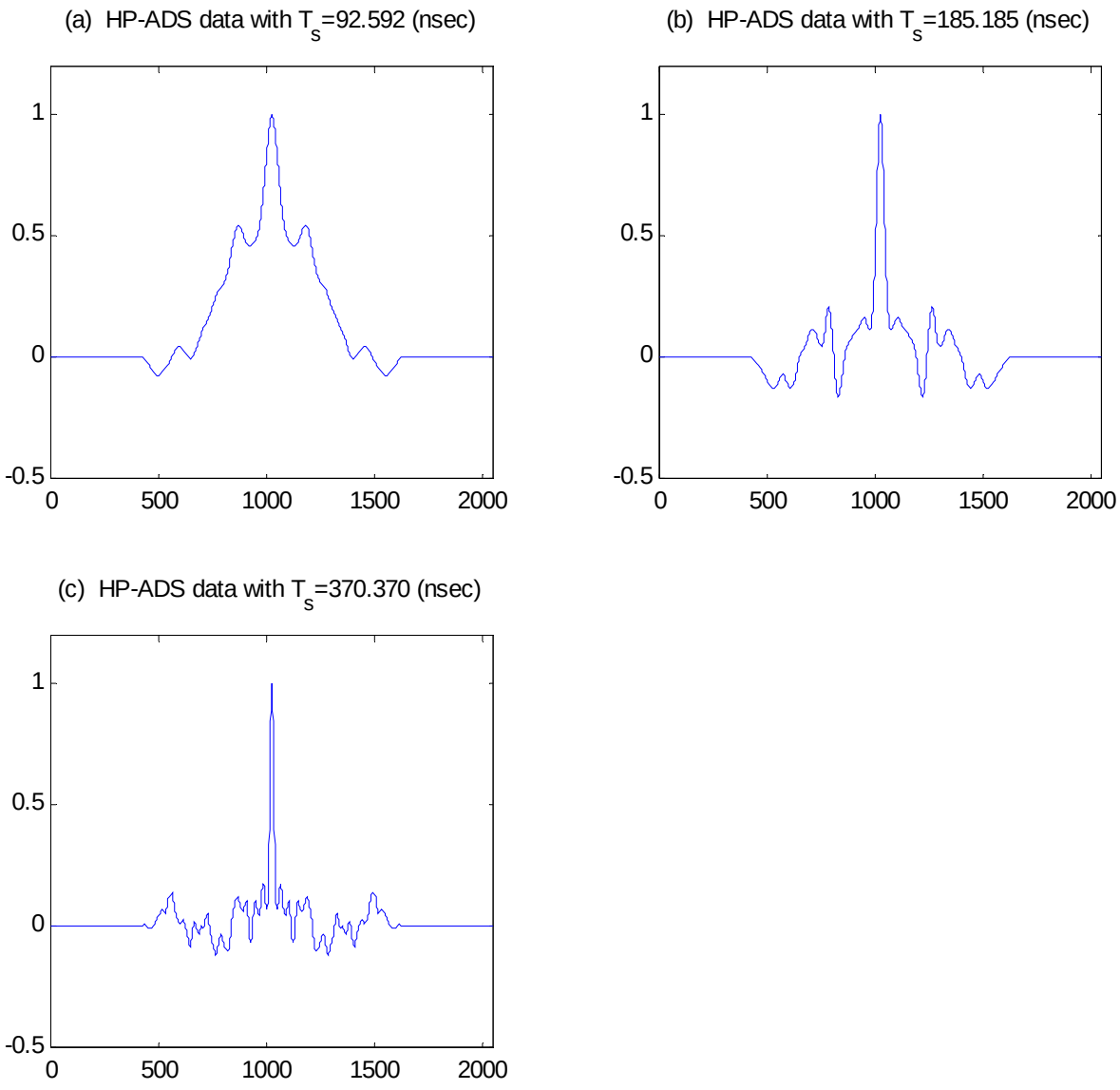

Figure 5.4. Auto-correlation of the HP-ADS GSM test signals

Note that a better correlation is observed with increase in the sampling interval. The main lobe is sharper, while the side lobes are reduced. This is a key point in the upcoming discussion regarding the results of our simulations.

B. JAMMING SIGNAL

In order to demonstrate the performance of the proposed denoising methods in a jamming environment, a noise jamming waveform is used.

The purpose of the noise jamming is to interfere with the enemy's electronic equipment so that the actual signal is distorted or over shadowed. The advantage of using noise jamming is that very little detail of the enemy's equipment needs to be known.

Based on information theory, the noise with a uniform spectral density, over the band of interest, provides one of the best noise-jamming waveforms. That is the white Gaussian noise, which has the maximum entropy, compared to other random waveforms, for a specified average power [23]. This characteristic makes it difficult to distinguish between receiver noise, in the victims system, and externally injected jamming noise.

The simplest method to generate a noise-jamming signal is high-power amplification of band limited Gaussian noise. This method is known as direct noise amplification (DINA) [23].

However, most of the high–power microwave amplifiers are limited in the peak power they can handle. For this reason, alternative and much more flexible methods have been established to generate high power noise. One of these utilizes frequency or phase

modulation of the jammer's signal, with a random waveform. The advantage of this method is that maximum output power can be obtained from the jammer transmitter.

Based on the above, we are using a jamming signal referred to as "erfed" FM noise [23]. A block diagram, shown in Figure 5.5, illustrates the principles of generating this type of noise to be used as jamming waveform.

Figure 5.5. Block diagram of Erfed FM noise generation

In Figure 5.5, a base band Gaussian frequency control waveform (noise) is applied to frequency modulate a power oscillator, such as a backward wave oscillator (BWO) or carcinotron microwave source. This allows the buildup of a Gaussian pseudo noise jamming waveform in the victim's receiver. In order to produce the desired uniform RF power spectrum at the output of the jammer, it is necessary to alter the amplitude distribution of the modulating noise before it is used to modulate the carrier [24]. It has been shown that the necessary transformation can be achieved with the use of a nonlinear network with transfer function the error function (erf()) [24]. That is why, the output waveform from the VCO, is called "Erfed" noise.

A MATLAB code is used to generate the desired jamming waveform. Two scenarios are simulated. One generates a jamming signal with a bandwidth equal to the bandwidth of the receiver (1.2 MHz) [22], while in the second; the jamming waveform

interferes only with the bandwidth of a physical channel, which is 200 KHz. The base band Gaussian noise source used in these scenarios has a bandwidth of 55 KHz, for the first scenario, and a 20 KHz, for the later.

Figures 5.6 (a) and 5.7 (a) show the Gaussian noise waveform for the two scenarios, while Figures 5.6 (b) and 5.7 (b) depicts their respective Power Spectral Densities (PSD). Figures 5.6 (c) and 5.7 (c) display the generated noise spectra for the two test cases, while Figures 5.6 (d) and 5.7 (d) show the time behavior of the jamming signal.

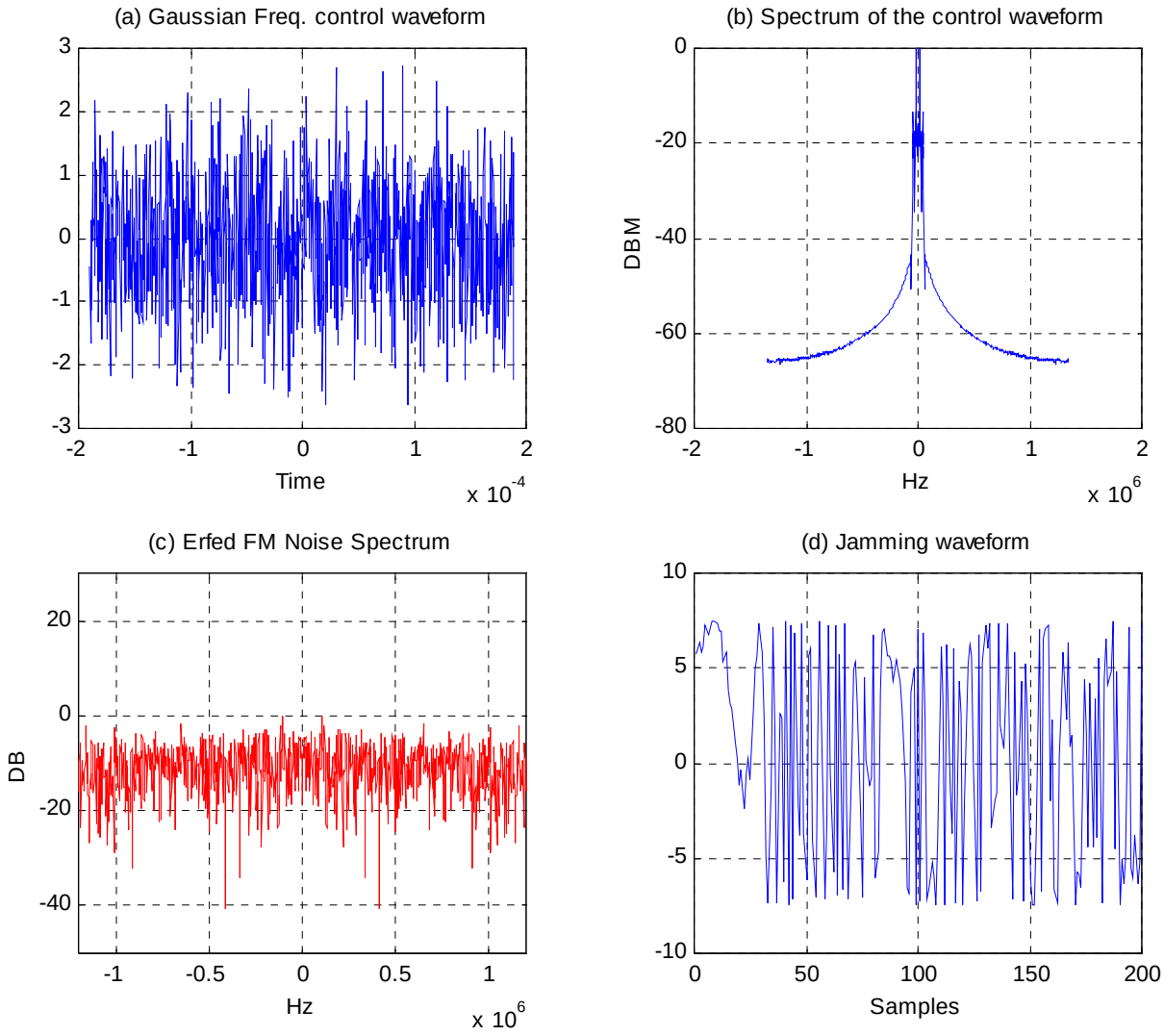

Figure 5.6. Erfed Jamming waveform with bandwidth 1.2 MHz

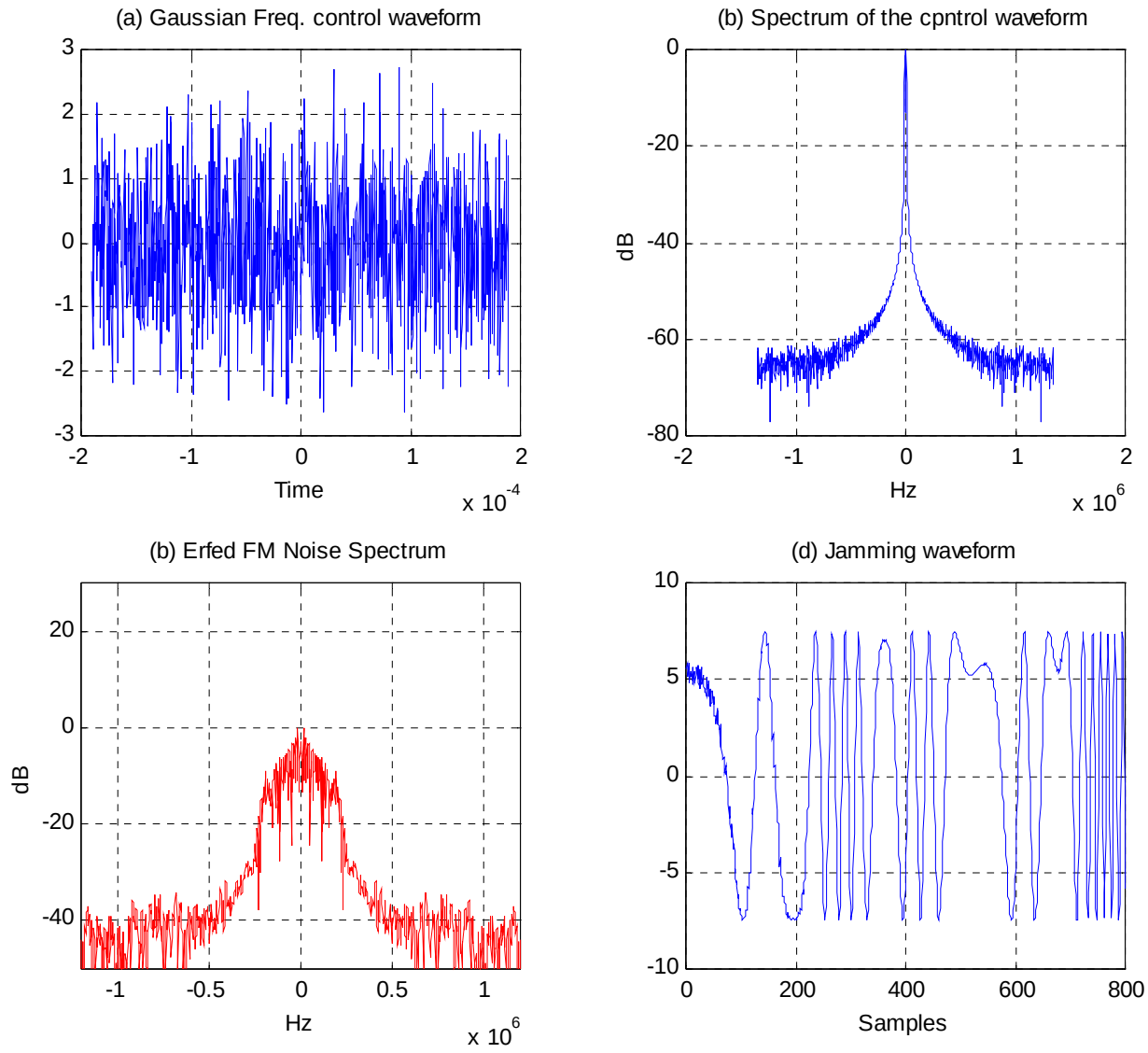

Figure 5.7. Erfed Jamming waveform with bandwidth 200 KHz

The detailed MATLAB code for the generation of the jamming waveforms is shown in Appendix [C].

THIS PAGE INTENTIONALLY LEFT BLANK

VI. SIMULATION RESULTS

A. UNEQUAL SNR CONDITIONS

In this section we apply the methods described in Chapter IV, to our test HP-ADS generated signals embedded in zero mean, white Gaussian noise.

Our goal is to investigate how well we can extract useful TDOA data. The Mean Squared Error (MSE) is used as the measure of improvement. We define the MSE as the square of the difference between he true TDOA value and the estimated TDOA value. We compare the MSE obtained from the proposed methods (improved value), to MSE for non-denoised TDOA estimation (original value).

Each of the proposed denoising methods is evaluated for each of the three sampling frequencies. For the convenience of the reader we label the test signals as follows:

(1) HP-ADS signal with sampling interval of 92.592 nsec.

(2) HP-ADS signal with sampling interval of 185.185 nsec.

(3) HP-ADS signal with sampling interval of 370.370 nsec.

All simulations were performed using MATLAB [25]. The codes used are provided in Appendix [C]. For lucidity in the following discussion, we define the percentage improvement and the average percentage improvement. The percentage improvement is given by

$$\text{Percentage improvement} = \frac{\text{MSE value without denoising} - \text{MSE value with denoising}}{\text{MSE value without denoising}} \times 100$$

The average percentage improvement is simply the mean value of the percentage improvement for all values of total SNR. True TDOA is randomly chosen between –150 to +150 samples, thus the MSE value represents the sample difference squared. To quantify the MSE further, consider for example a value of 4. This value corresponds to a sample difference of 2 and hence a time delay of 2x(Sampling Interval (nsec)). The transforms use a Daubechies wavelet of order 8 (i.e., db4 [26, 27]), and the optimum level of decomposition was determined, by trial and error, to be 5. Unequal levels of noise are used in each channel, and the lowest SNR value (limit) is obtained, that still permits reasonable localization. Reasonable localization provides a MSE smaller than that obtained by using raw data. A fixed value of SNR ranging from 3 dB down to –9 dB, is kept in one channel while the SNR values in the other channel are varied [28]. The signal power is unity and different SNRs, are obtained by scaling the random noise sequences. The MSE versus the total SNR in both channels is plotted. The total SNR represents the sum of the SNR values of the two channels. The results are shown in Figures 6.1, 6.2 and 6.3. Figures 6.1(a), 6.2(a), and 6.3(a) depict the region of the SNRs over which we have results that permit reasonable localization, while Figures 6.1(b), 6.2(b) and 6.3(b) show the limiting cases (lowest SNR in each channel).

One obvious trend is that the MSE improves, i.e., decreases, as the sampling interval increases. This observation is also evident in Tables 6.1 and 6.2, which contain the numerical values of the computed MSE for each test signal as obtained by using the MAML method and the Modified Fourth Order Moment (MFOM) method, respectively.

In both tables, we can clearly see a decrease in error values as we move across each row from left to right. Note that in Table 6.1 and for the MAML case for data with sampling interval 185.185 (nsec), a small inconsistency exists.

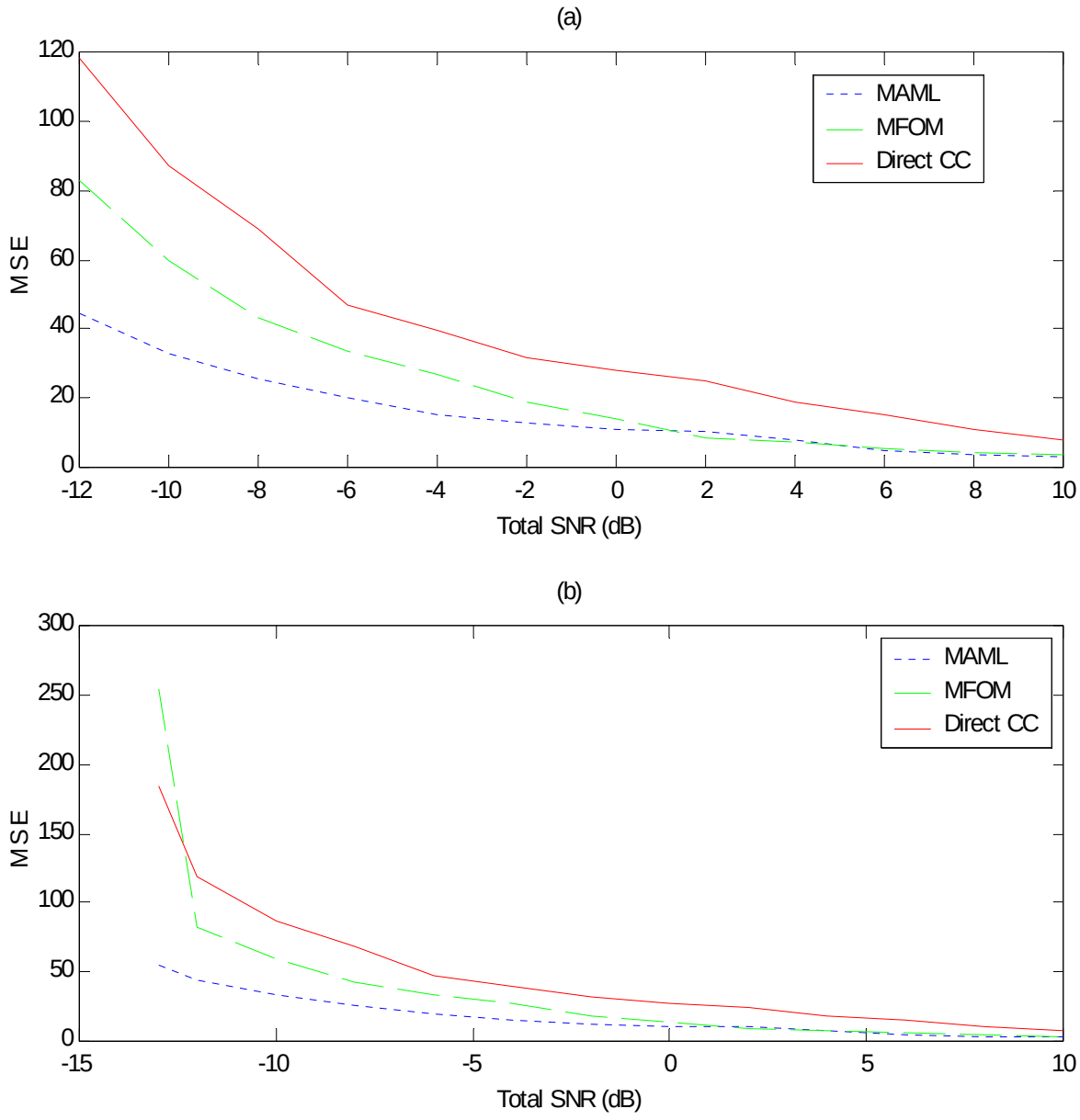

Figure 6.1. MSE versus total SNR for HP-ADS data with T_s=92.59 (nsec)

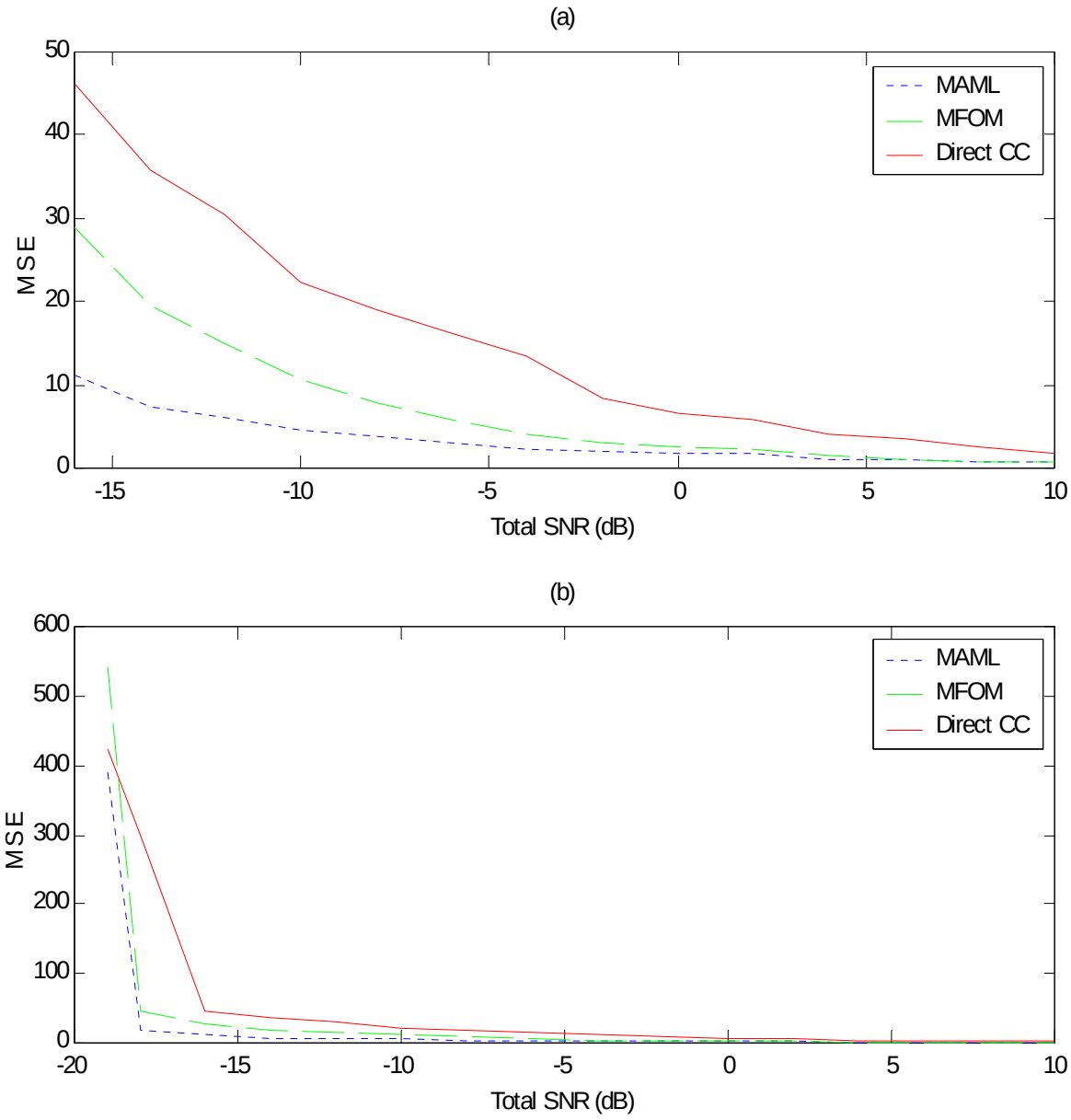

Figure 6.2. MSE versus total SNR for HP-ADS data with T_s=185.185 (nsec)

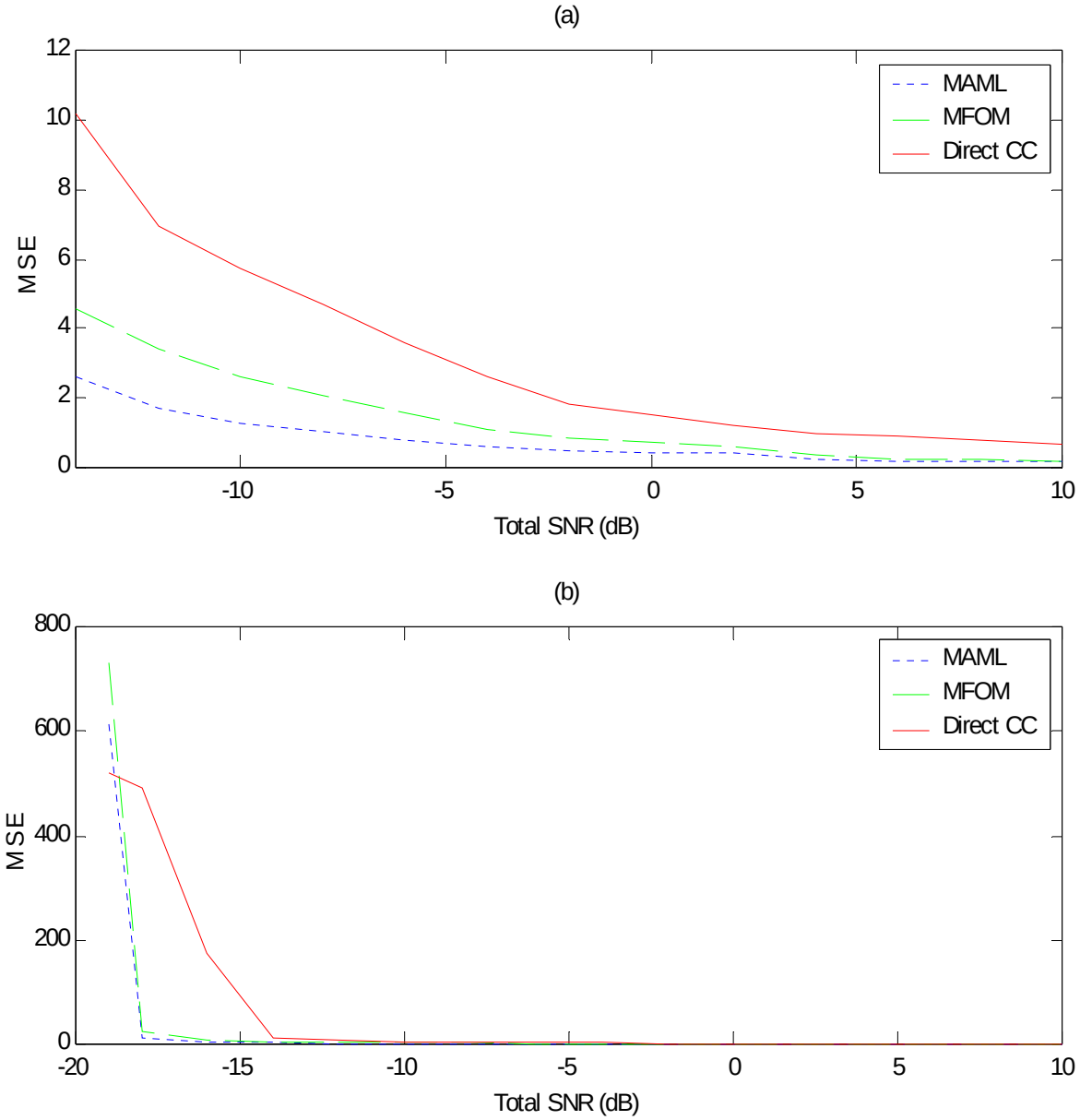

Figure 6.3. MSE versus total SNR for HP-ADS data with T_s=370.370 (nsec)

Total SNR in (dB)	Mean Squared Error (MSE)					
	Sampling Interval 92.59 (nsec)		Sampling Interval 185.185 (nsec)		Sampling Interval 370.370 (nsec)	
	Non Denoised	MAML	Non Denoised	MAML	Non Denoised	MAML
10	8.20	3.00	1.83	0.71	0.67	0.17
8	10.92	3.69	2.65	0.71	0.79	0.17
6	15.92	5.10	3.50	0.90	0.88	0.18
4	19.03	8.04	4.05	1.10	0.98	0.22
2	24.78	10.33	5.73	1.79	1.22	0.45
0	28.07	10.95	6.50	1.78	1.52	0.46
-2	31.78	12.74	8.36	1.92	1.83	0.51
-4	39.56	15.51	13.41	2.31	2.60	0.61
-6	46.79	20.04	16.15	3.16	3.62	0.80
-8	68.81	25.50	18.98	3.76	4.69	1.00
-10	87.38	33.07	22.38	4.64	5.72	1.27
-12	118.18	44.19	30.52	6.13	6.93	1.72
-14			35.80	7.33	10.19	2.63
-16			46.22	11.11	174	4.38
-18			297	17.87	492	12.25

Table 6.1. MSE values at different values of total SNR for MAML method

Total SNR in (dB)	Mean Squared Error (MSE)					
	Sampling Interval 92.59 (nsec)		Sampling Interval 185.185 (nsec)		Sampling Interval 370.370 (nsec)	
	Non Denoised	MFOM	Non Denoised	MFOM	Non Denoised	MFOM
10	8.20	3.52	1.83	0.65	0.67	0.19
8	10.92	4.07	2.65	0.81	0.79	0.22
6	15.92	5.68	3.50	1.07	0.88	0.27
4	19.03	7.05	4.05	1.51	0.98	0.36
2	24.78	8.59	5.73	2.18	1.22	0.63
0	28.07	14.03	6.50	2.62	1.52	0.73
-2	31.78	18.95	8.36	3.12	1.83	0.76
-4	39.56	26.79	13.41	4.10	2.60	1.10
-6	46.79	33.41	16.15	5.76	3.62	1.60
-8	68.81	43.08	18.98	7.92	4.69	2.06
-10	87.38	59.87	22.38	10.66	5.72	2.65
-12	118.18	82.68	30.52	15.01	6.93	3.43
-14			35.80	19.62	10.19	4.55
-16			46.22	28.91	174	7.75
-18			297	46.65	492	25.12

Table 6.2. MSE values at different values of total SNR for the Modified Fourth Order Moment method

This is the value of 1.79 observed at 2 dB total SNR, which is greater than the 1.78 observed at 0 dB of total SNR. This may be due to the random number generator we use to generate the noise sequences, or to the number of the realizations (100 realizations) for the simulations purposes. An increase in the number of the simulation repetitions, may remove this inconsistency.

The limits obtained for each method and for each sampling rate are given in Table 6.3.

Sampling Interval (nsec)	**Lowest SNR allowed in each channel (dB)**		**Maximum difference in SNR between the two channels (dB)**	
	MAML	Modified 4^{TH} Order Moment	MAML	Modified 4^{TH} Order Moment
92.59	-8	-6	14	12
185.185	-9	-8	18	17
370.370	-9	-9	20	18

Table 6.3. Limitations in SNR values

The limiting cases represent the threshold below that the denoising methods do not perform well. The MSE in these cases, appear to have larger values than the non-denoised MSE values, as computed by the direct cross-correlation of the raw data.

An important fact is that in addition to the limits of the lowest SNR in each channel, there is also a restriction regarding the combination of the SNRs in the channels, that is the total SNR. For example, consider a value of –3 dB for total SNR. This can be

achieved by a large number of combined values of SNRs in each channel. But not all of the combinations are allowed; only the ones that have a dB separation smaller than the maximum difference. This maximum difference is found to be as shown in the last two columns of Table 6.3. Again we see that this limit increases as the sampling interval increases. The MAML method appears to permit a larger number of SNR combinations to achieve a specific total SNR value compared to the MFOM method.

Interpreting Figure 6.1(a), we see that using the HP-ADS data with a sampling interval of 92.59 (nsec), the average percentage improvement over all total SNR values between –12 and 10 dB is about 61.53% for the MAML method, and 46.71% for the MFOM method.

The HP-ADS data with a sampling interval 185.185 (nsec), see Figure 6.2(a), permits an average percentage improvement, over all total SNRs between –18 and 10 dB, of 76% when MAML denoising is applied, and 60.5% when the Modified Fourth Order Moment denoising is used.

The average percentage improvement for the HP-ADS data with a sampling interval of 370.37 (nsec), see Figure 6.3(a), is even better. In this case we obtain improvements of 78% and 63.3% for the MAML and the Modified Fourth Order Moment, respectively, over total SNR values between –18 and 10 dB. The MSE for all methods and for all SNRs above a total of 10dB is essentially zero, provided each channel has an SNR above the lowest SNR value shown in Table 6.3.

The improvements we discussed above can also be related to the plots in Figure 5.4, which presents the auto-correlation function of the test signals. There, we observed improved correlation with decreasing sampling frequency.

Hence we can state that a higher degree of correlation of the signal components reduces the probability of error in the TDOA estimation.

B. PERFORMANCE IN A JAMMING ENVIRONMENT

In Chapter IV, we discussed in detail two denoising methods to improve TDOA estimates. In this section, we will use these methods to test the performance for the HP-ADS generated signals embedded in Gaussian white noise subject to a jamming signal, as described in Chapter V.

Again, the goal is to investigate how well useful TDOA information can be extracted. The mean squared error (MSE) is the measure of improvement, i.e., the lower MSE the better the TDOA estimate.

We define the percentage degradation of the MSE, and the average percentage degradation, in an analogous way as for the percentage improvement. The corresponding formula is

$$\text{Percentage degradation} = \frac{(\text{MSE value without Jamming}) - (\text{MSE value when Jamming present})}{(\text{MSE value without Jamming})} \text{x}100$$

Each denoising method is tried in two jamming scenarios, as described in Chapter V, for each of the three HP-ADS data sets. We will only present the case in which the

full bandwidth of the receiver is jammed, since the other case follows a similar trend. The results and the related plots of the latter case can be found in Appendix [B].

The labeling of the test signals is kept as in the previous section. For the jamming simulations, each channel uses equal SNR levels. The values of SNRs, used in both channels, range from 20 dB to –6 dB. Four values of jamming-to-signal (J/S) ratios are used, 10 dB, 5 dB, 0 dB, and –10 dB. These values are obtained by proper scaling of the jamming waveform.

The MSE versus SNR in each channel is plotted, with the jamming-to-signal ratio as a constant parameter. The results are obtained using 100 realizations for each SNR, and are shown in Figures 6.5, 6.6, and 6.7.

Figure 6.4 shows the performance of the denoising methods when no jamming is present. This provides a reference for how the denoising performs in a jamming free environment. Notice that the MSE improves (decreases), as the sampling frequency decreases and that the MAML method outperforms the Modified Fourth Order Moment method in all cases.

The improvements can also be seen in Table 6.4, which contains the average percentage improvement computed for each method and each sampling interval.

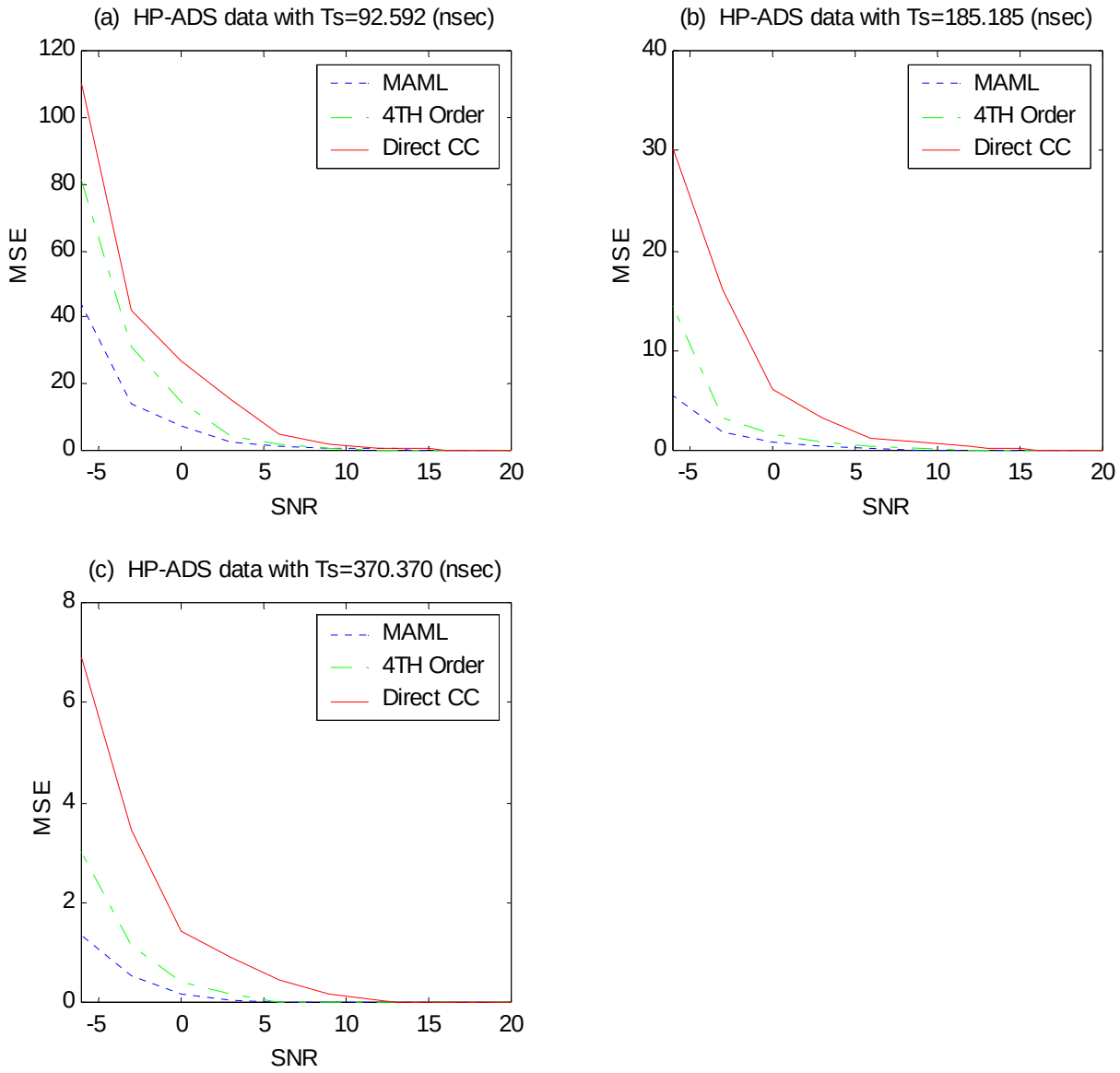

Figure 6.4. MSE versus SNR for the HP-ADS data, when jamming is not present

	Average Percentage Improvement %		
	Sampling Interval 92.59 (nsec)	Sampling Interval 185.185 (nsec)	Sampling Interval 370.370 (nsec)
MAML method	70.4	88.63	91.37
MFOM method	62	77.14	79

Table 6.4. Average percentage improvement in MSE, when jamming is not present

The improvement in MSE is related to the sampling frequency and is related to the degree of correlation of the signal components. Improved correlation reduces the probability of error in the TDOA estimation.

Continuing the discussion, lets take a look at Figures 6.5, 6.6, and 6.7. Each figure represents the results of denoising when jamming is present in one channel, for the HP-ADS data with sampling interval 370.370 (nsec), 185.185 (nsec), and 92.59 (nsec), respectively.

We see that the MSE improves (decreases) as the sampling interval increases, or when the jamming-to-signal ratio decreases. It is obvious that higher levels of jamming power present in our signals degrade the performance of the denoising methods. The quality of MSE estimates degenerates as the power of the jammer increases. Also the SNR range, in which reasonable estimates are obtained, decreases as the J/S ratio increases.

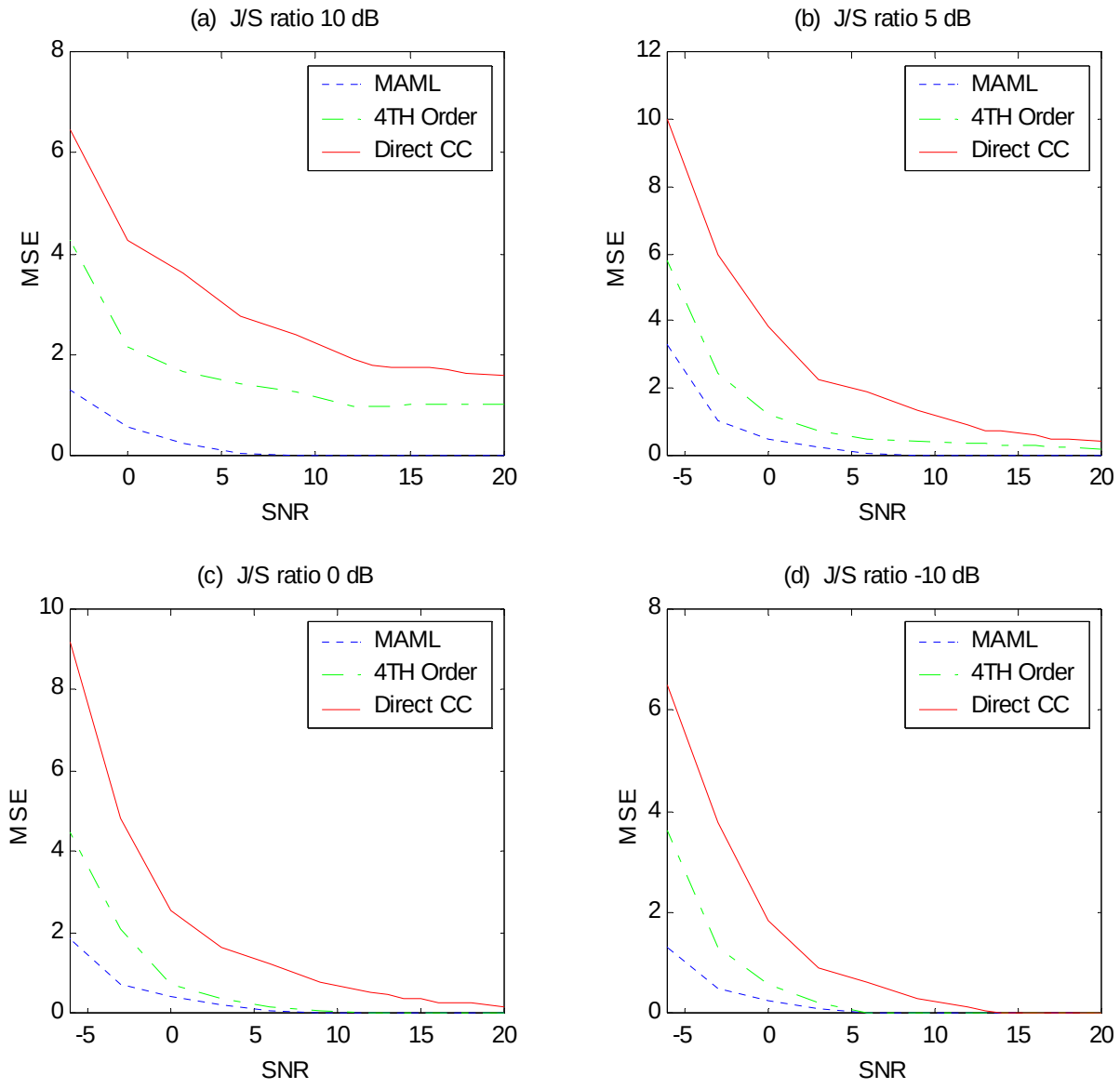

Figure 6.5. MSE versus SNR for HP-ADS data with T_s=370.37 (nsec), at different J/S ratios

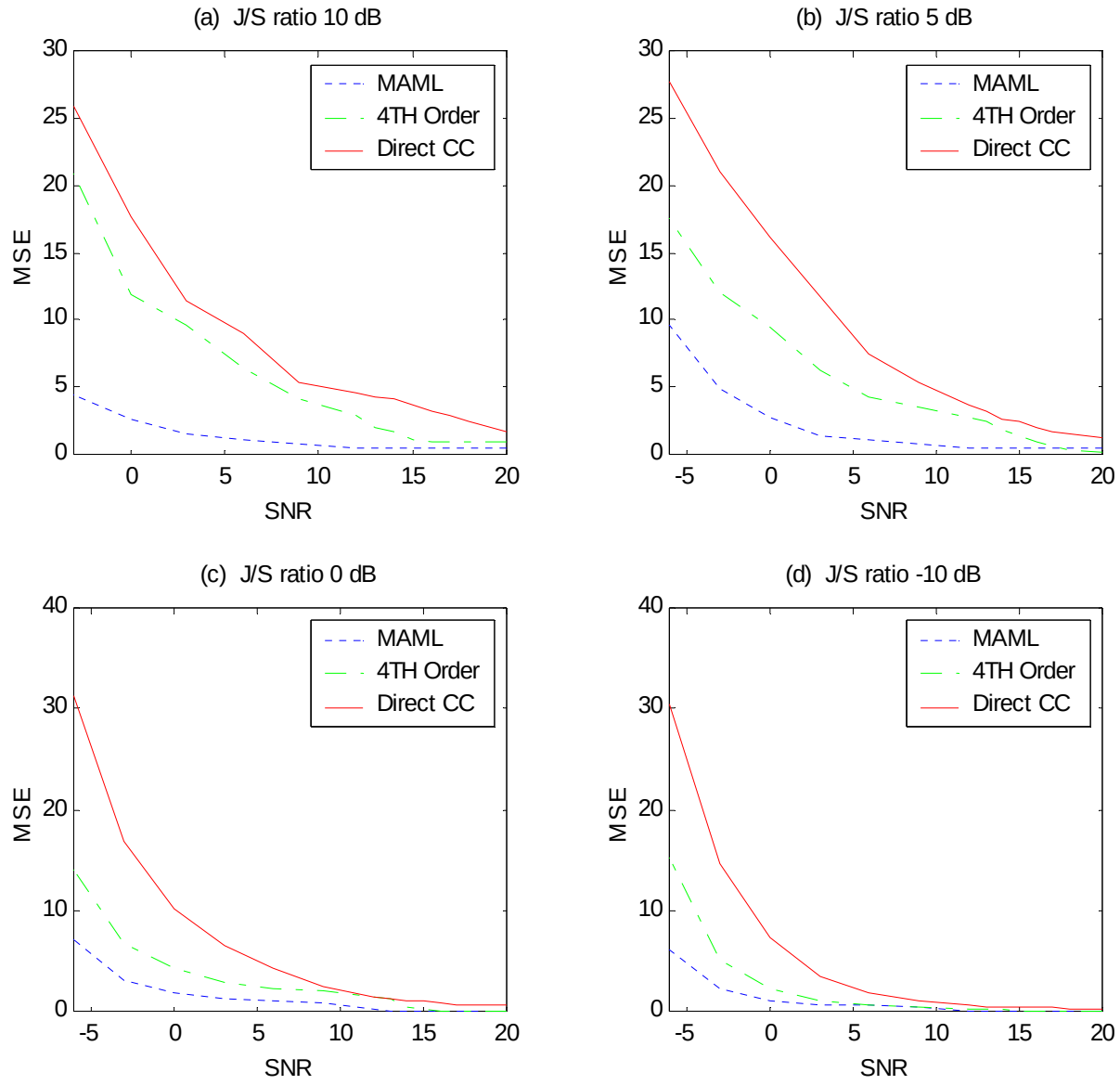

Figure 6.6. MSE versus SNR for HP-ADS data with T_s=185.185 (nsec), at different J/S ratios

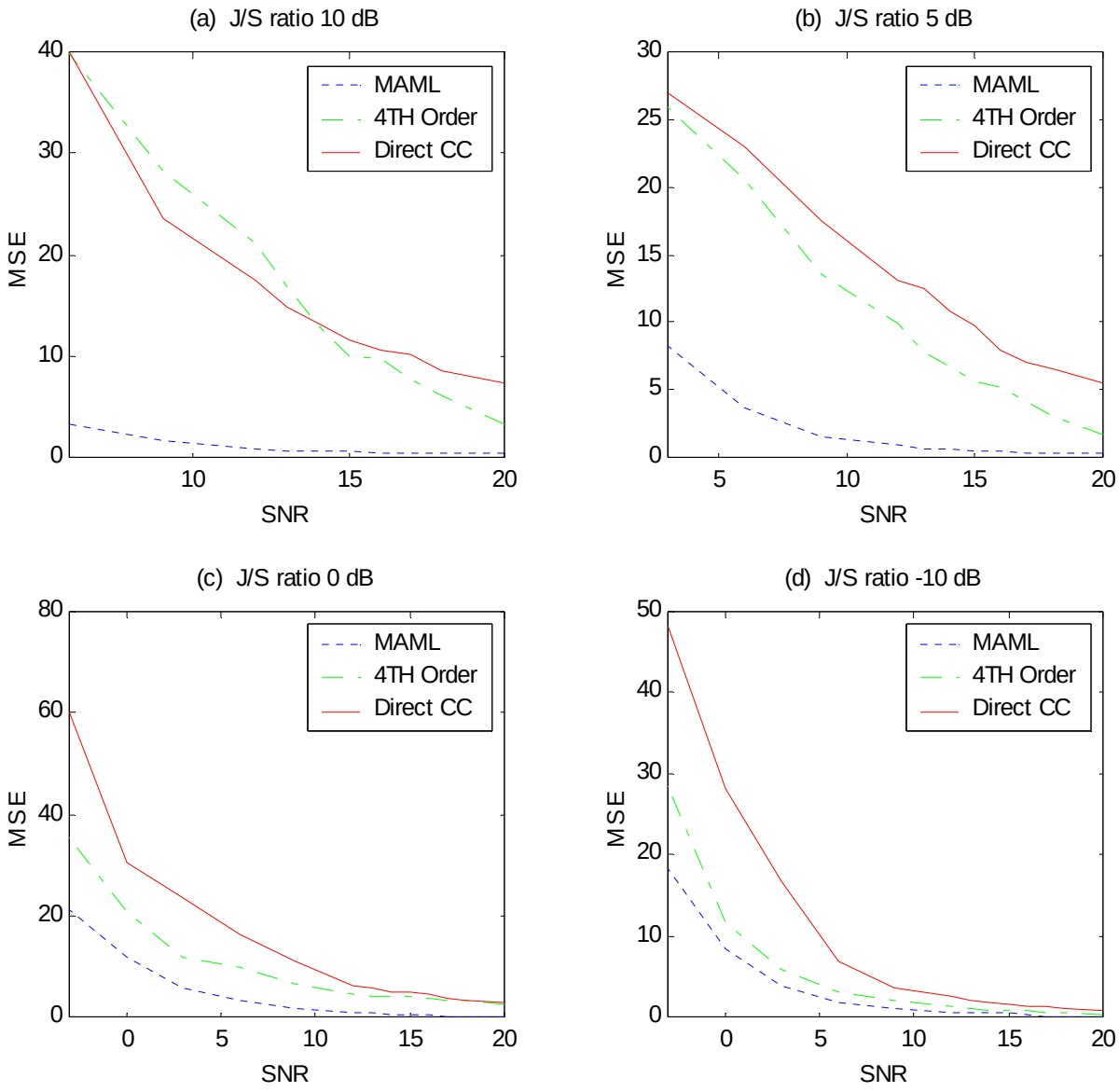

Figure 6.7. MSE versus SNR for HP-ADS data with T_s=92.592 (nsec), at different J/S ratios

Specifically, using the HP-ADS data, with a sampling interval of 370.370 (nsec) (see Figure 6.5(a)) provides reasonable estimates above –3 dB for a 10dB jamming-to-signal ratio. Figures 6.5(b-d) allow reasonable MSE values for SNR's greater than –5 dB. Table 6.5 contains the average percentage degradation of the computed MSE for different values of J/S ratios, as compared to the MSE obtained when no jamming is present.

Jamming-to-signal ratio (dB)	**Average Percentage Degradation %**	
	MAML method	Modified 4^{TH} Order Moment method
10	73.98	88.71
5	70.05	78.91
0	60.05	65.24
-10	28.30	33.97

Table 6.5. Average percentage degradation in MSE at various J/S ratios (HP-ADS data with sampling interval 370.370 (nsec))

We also see that using the MAML method at a 10dB J/S ratio, the MSE values are on average, 73.98% worse than those obtained when no jamming is present. The MFOM method gives MSE values that are 88.71% worse for the same J/S ratio. It is evident that the MAML method outperforms the Modified Fourth Order Moment method, since it

gives MSE values which on average are better (relative to the no jamming situations) than those obtained using the MFOM method.

For the HP-ADS data with a sampling interval of 185.185 (nsec) the results are shown on Figure 6.6(a-d) and the computed average percentage degradation is given in Table 6.6.

Jamming-to-signal ratio (dB)	**Average Percentage Degradation %**	
	MAML method	Modified 4^{TH} Order Moment method
10	78.50	93.68
5	76.74	90.69
0	68.30	81.60
-10	48.68	54.36

Table 6.6. Average percentage degradation in MSE at various J/S ratios (HP-ADS data with a sampling interval of 185.185 (nsec))

In this case, we observe that the presence of jamming limits the SNR value in the channels to be larger than –3 dB and in addition, we see an increased average percentage degradation, relative to the values of Table 6.5.

The average percentage degradation at 10dB J/S ratio is 78.5% using the MAML method, and 93.68% when the MFOM method is applied. Still, the MAML method gives

better results than the MFOM method, but the performance is reduced as the sampling frequency is increased.

The HP-ADS data with a sampling interval 92.59 (nsec), see Figure 6.7(a-d), provides the worst MSE values. In this case, the presence of jamming severely affects the extraction of reasonable estimates. The SNR range is required to be larger than 6 dB when the J/S ratio is 10 dB, see Figure 6.7(a), while we require a 3 dB SNR in each channel when J/S ratio is 5 dB or less, see Figure 6.7(b). Table 6.7 shows the percentage degradation of MSE, based on the minimum SNR in each channel.

Jamming-to-signal ratio (dB)	**Average Percentage Degradation %**	
	MAML method	Modified 4^{TH} Order Moment method
10	72.28	98.78
5	69.68	97.58
0	65.41	94.75
-10	55.54	80.17

Table 6.7. Average percentage degradation in MSE at various J/S ratios (HP-ADS data with sampling interval 92.59 (nsec))

Considering the results presented in Tables 6.5, 6.6, and 6.7, we can say that the increase in sampling frequency reduces the quality of the TDOA estimation (compare the average degradation performance, under the same J/S ratio, of different sampling

intervals). In addition we observe that the MAML method out performs the MFOM method in all cases (in each Table MAML gives better results than the MFOM method does). The MAML method also appears to be more robust in a jamming environment, since the degradation of the computed MSE values, at various J/S ratios, deviates less, as compared to MFOM method. For example, from Table 6.6, we see that the average degradation computed, when MAML method is applied, extends from 48.68% up to 78.5%, for –10 dB up to 10 dB J/S, while the MFOM method has a range from 54.36% up to 93.68%.

The previous observations for the performance of the denoising methods, are also verified if we consider the improvement of the MSE values computed from the denoised data as compared to the ones obtained by the direct cross-correlation.

In Table 6.8 the average percentage improvement of the MSE is summarized for the three data sets at each jamming-to-signal ratio. Note that the average SNR improvement values of the HP-ADS data set with the sampling interval 92.59 (nsec) appears to be inconsistent, if we consider the observations we have made so far. This is not true, because in this case, the computed values of the mean squared error are based upon a smaller range of SNRs (we are limited in SNR according to the J/S ratio). The improvement in this case must be quantified by taking the smaller SNR range into account.

Jamming-to-signal ratio (dB)	**Average Percentage Improvement %**					
	Sampling Interval 370.370 (nsec)		Sampling Interval 185.185 (nsec)		Sampling Interval 92.59 (nsec)	
	MAML	Modified 4^{TH} Order Moment	MAML	Modified 4^{TH} Order Moment	MAML	Modified 4^{TH} Order Moment
10	84	44.20	82.40	45.82	(20 dB down to 6dB SNR) 89.8	(20 dB down to 6dB SNR) 7.88
5	86.50	58.71	83.65	47.05	(20 dB down to 6 dB SNR) 92	(20 dB down to 6 dB SNR) 37.27
0	88.60	77.94	86.10	54.24	(20 dB down to 3 dB SNR) 85.34	(20 dB down to 3 dB SNR) 41.13
-10	90.60	78.74	86.90	64.49	(20 dB down to 0 dB SNR) 77.46	(20 dB down to 0 dB SNR) 51.28

Table 6.8. Average percentage improvement in MSE when Jamming is present

THIS PAGE INTENTIONALLY LEFT BLANK

VII. SUMMARY, CONCLUSIONS AND FUTURE WORK

A. SUMMARY AND CONCLUSIONS

This thesis is focused on the improvements made possible by denoising, in conjunction with wavelet processing, for estimating the Time Difference Of Arrival (TDOA) of GSM signals received at two spatially separated sensors.

Two wavelet based denoising methods are proposed to improve the TDOA estimation: the Modified Approximate Maximum Likelihood (MAML), and the Modified Fourth Order Moment (MFOM) method.

The performance of these methods was evaluated under unequal SNR conditions as well as when jamming was present. The GSM signals used were generated with the help of the HP-ADS software. The Mean Squared Error (MSE) was used as criteria of goodness (low MSE denotes a small error and hence good localization).

The study indicates that the application of the denoising method improves the TDOA estimation, as compared to when no denoising is applied to the received signals. In particular, the MAML method allows a 70.4 to 91.37 percent improvement in the TDOA estimation, while the respective improvement obtained when the MFOM method is applied, ranges from 62 to 79 percent. Increasing the sampling interval over which signal samples are taken from the signal decreases the MSE.

In addition, we observed that the MAML method provided the best results, and outperformed the MFOM method, in all cases. The low SNR limits in each channel, above which denoising is beneficial were obtained. The MAML method appeared to be

more robust in presence of Gaussian noise and jamming, while the MFOM method shows an undesirable "sensitivity" at the lower SNR levels (i.e., below –3 dB).

B. FUTURE WORK

Follow on work should examine the possibility for a modification of the proposed algorithms, so that the time-varying characteristics of the signal can be accounted for.

In addition, the performance of the proposed denoising methods should be investigated under the presence of a fading environment, and/or when other jamming schemes are applied (which may be more effective or severe), than the "erfed" FM noise we used.

Finally, one could further quantify the results of our work by relating the MSE improvement to the proper solution of the hyperbolic equations as presented in Chapter III.

APPENDIX A. SIMMULATION RESULTS OF THE COMBINED DENOISING METHODS

As mentioned in Section IV.C, combinations of the proposed denoising methods were tried, see Figure 4.3, to obtain their performance in a noisy environment. Figures A.1, A.2, and A.3, present the results of our simulations when we apply the combined methods (MAML/MFOM and MFOM/MAML), on the three HP-ADS GSM signals, embedded in noise. We use the same SNR in both channels, in a range from 20 dB to –6 dB, and again the MSE stands as criteria of goodness (i.e. low MSE denotes a small error and hence good localization).

Each figure, one for each of the HP-ADS data sets, depicts the MSE, obtained using the combined methods, versus SNR, and also includes the MSE values obtained when each denoising method (MAML or MFOM), is applied individually. The reader can easily compare the performance of the combined methods in this way.

We have to point out that, from Figures A.1(c), A.2(c), and A.3(c), one can see that the combination of the MAML/MFOM performs better than the MFOM alone. So we can use this combination instead of the MFOM. But this is not what we did. The reason is obvious if we take a look at Figure A.4 (a-d). This figure presents the results for MSE versus SNR, in the range of 20 dB to –6 dB for the HP-ADS data with a sampling interval T_s=92.59 (nsec). It is clear that reasonable results using the MAML/MFOM combination are available for SNR values greater than –3 dB. It appears that the combined method can not perform well for low SNR values when the sampling

interval decreases, while the individually applied MFOM permits the extraction of reasonable MSE values, even in SNRs lower than –3 dB.

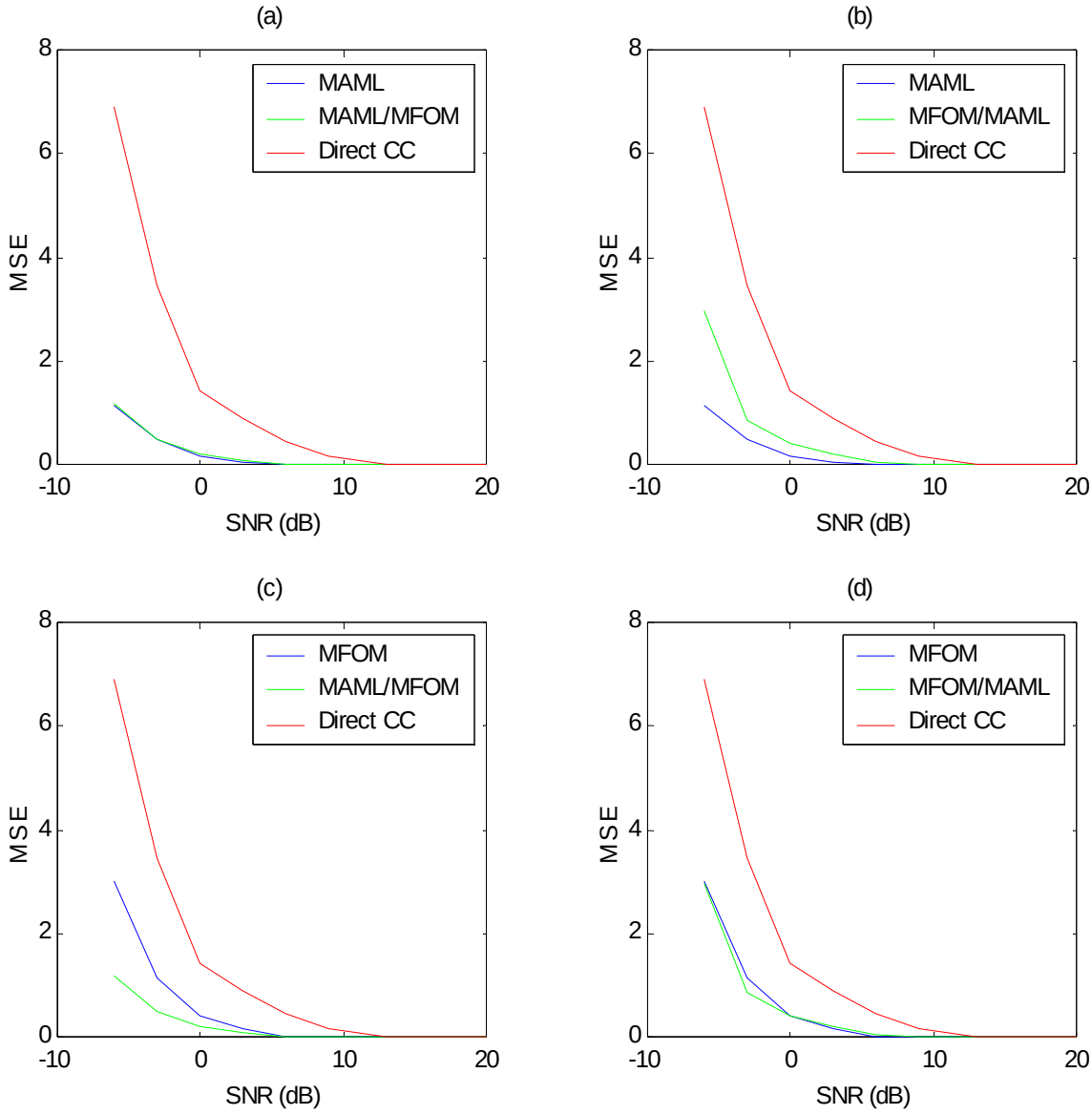

Figure A.1. Combined denoising methods as compared to the MAML method and the MFOM method for the HP-ADS data with T_s=370.37 (nsec)

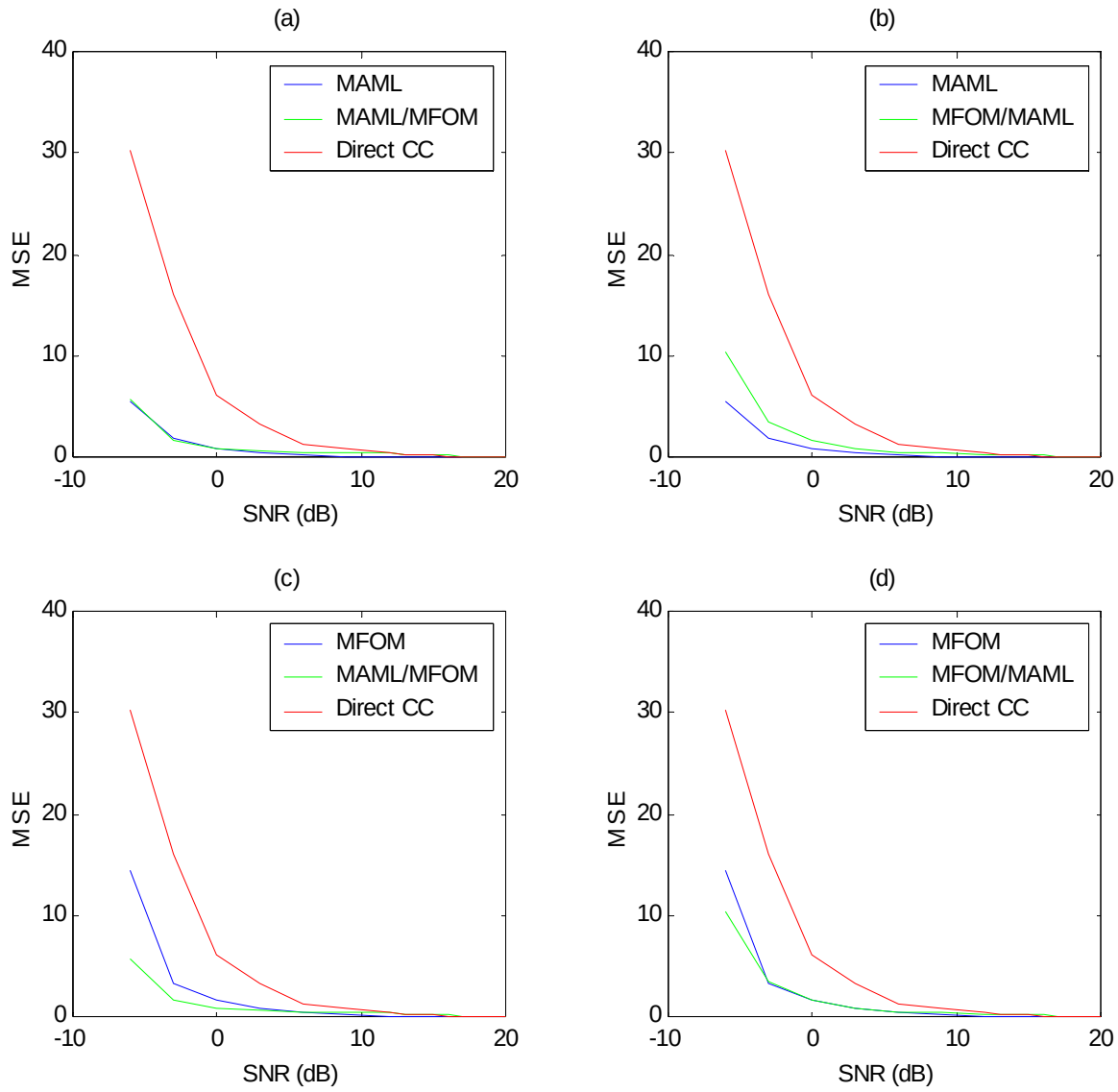

Figure A.2. Combined denoising methods as compared to the MAML method and the MFOM method for the HP-ADS data with T_s=185.185 (nsec)

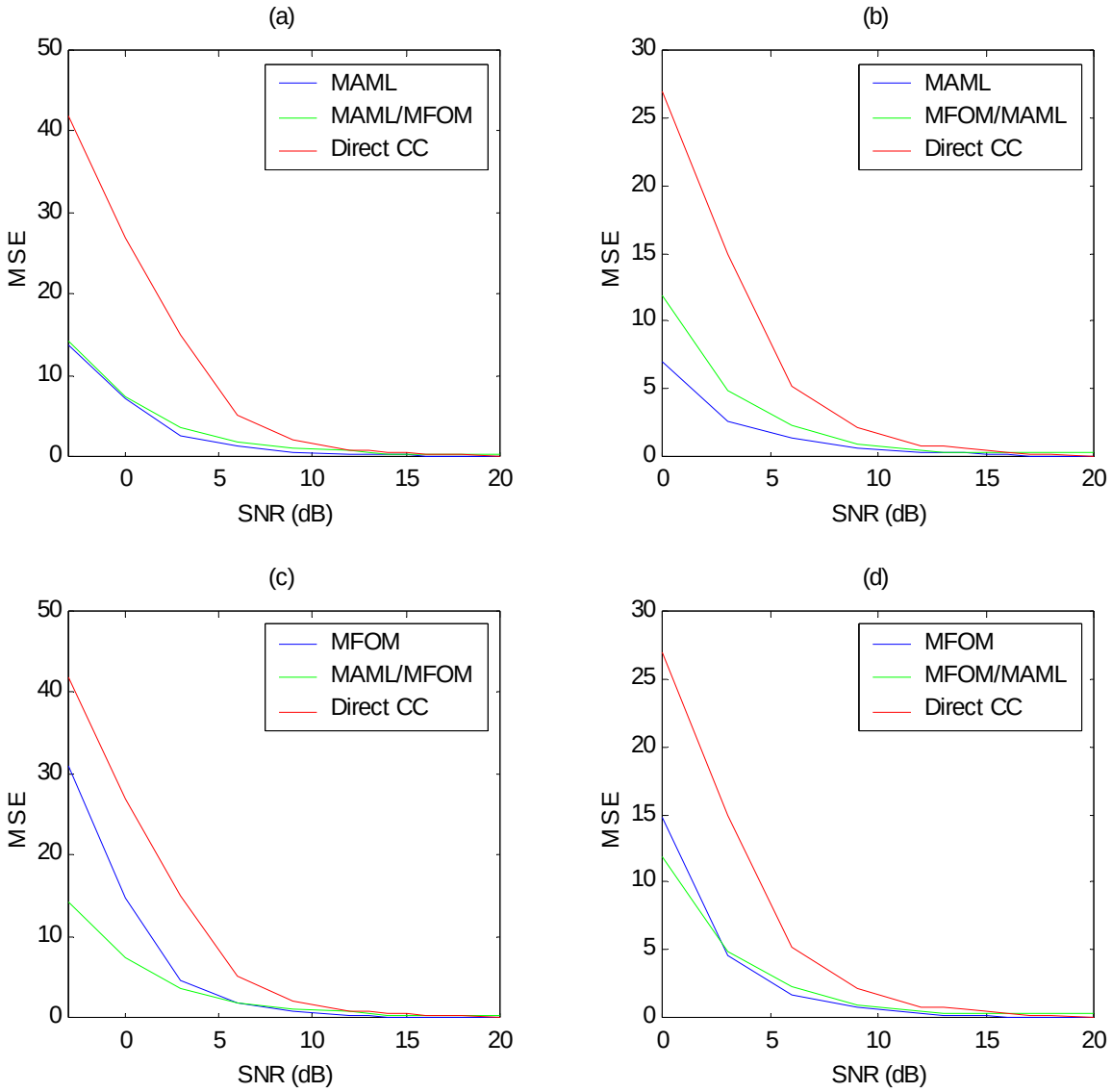

Figure A.3. Combined denoising methods as compared to the MAML method and the MFOM method for the HP-ADS data with T_s=92.59 (nsec)

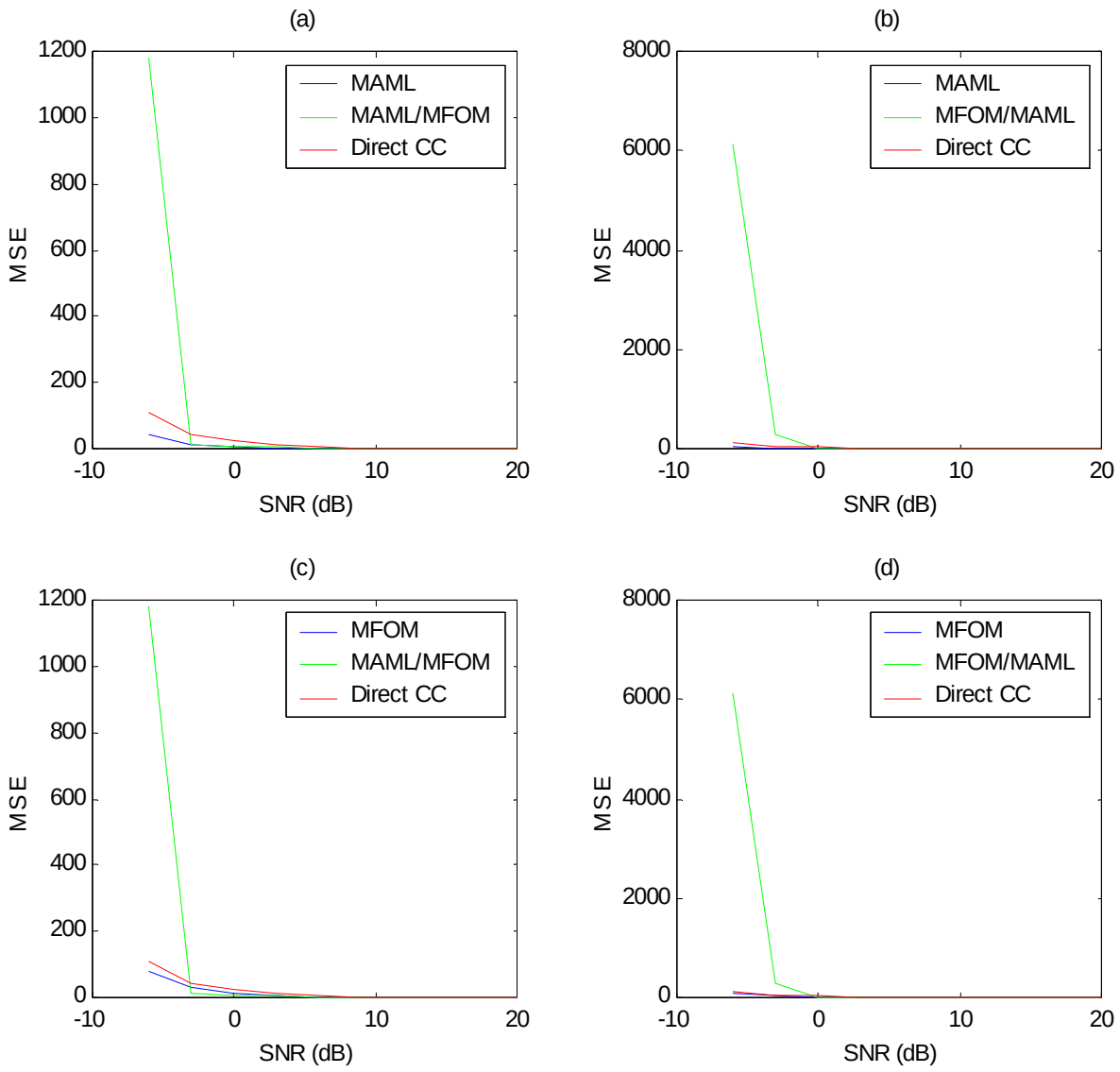

Figure A.4. Combined denoising methods as compared to the MAML method and the MFOM method for the HP-ADS data with T_s=92.59 (nsec) at a range of SNR values from 20 dB to –6 dB

THIS PAGE INTENTIONALLY LEFT BLANK

APPENDIX B. PERFORMANCE IN A JAMMING SITUATION (SCENARIO WITH 200 KHZ JAMMING BANDWIDTH)

A. RESULTS OF JAMMING FOR HP-ADS DATA WITH T_S=370.37 (NSEC)

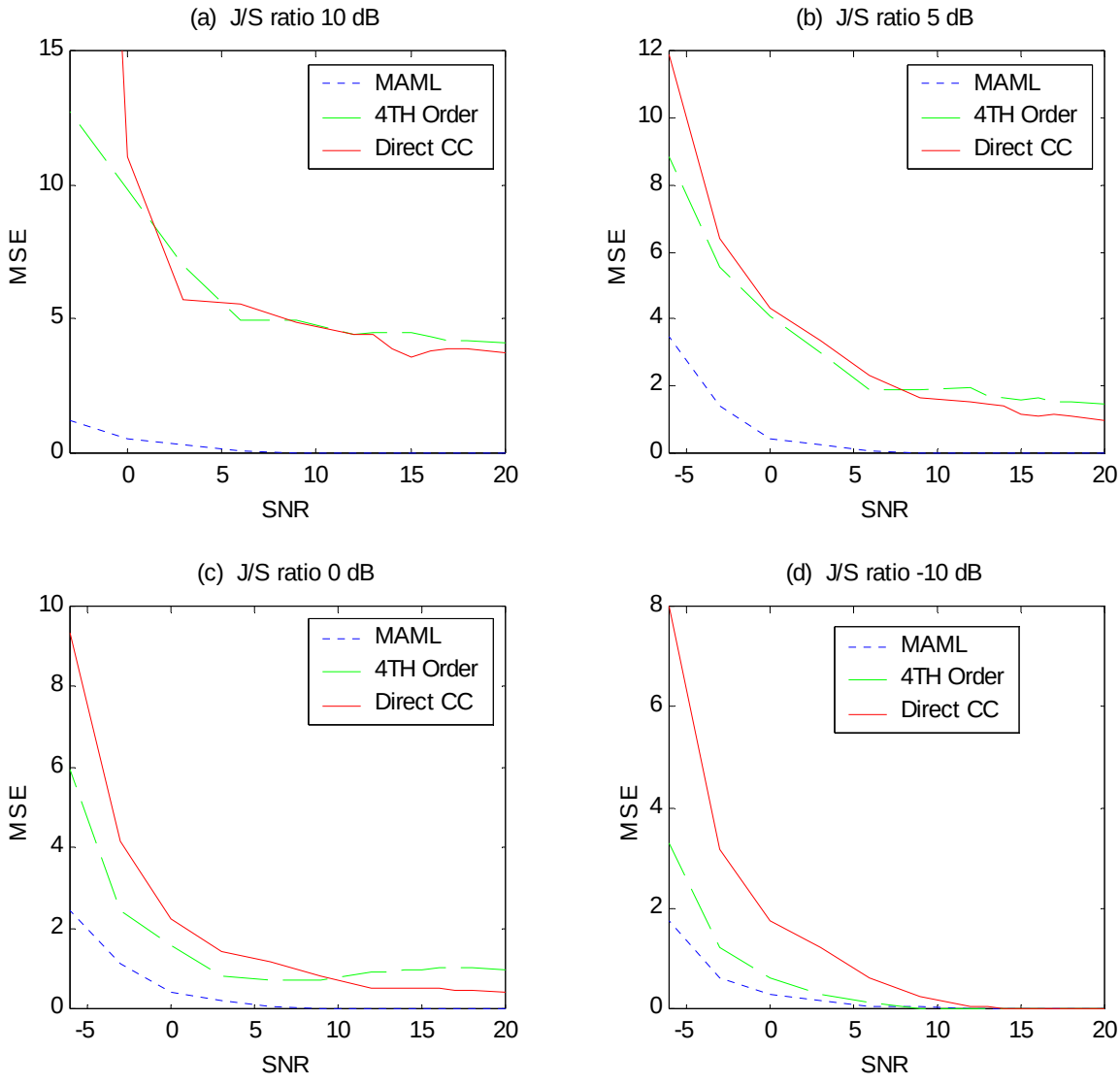

Figure B.1. MSE versus SNR at different jamming-to-signal (J/S) ratios (data with T_s=370.370 (nsec))

Jamming-to-signal ratio (dB)	**Average Percentage Degradation % for HP-ADS data with sampling Interval 370.37(nsec)**	
	MAML method	Modified 4^{TH} Order Moment method
10	76.01	96.86
5	73.12	92.60
0	69.32	81.10
-10	54.34	56.60

Table B.1. Average percentage degradation in MSE at various jamming-to-signal ratios (J/S)

As we can see from Figure B.1 and Table B.1, the conclusions discussed in Section VI.B are also applicable to the current situation. In this case where a more severe jamming situation is present, the denoising methods provide improved results. The MAML method outperforms the MFOM method and appears to be more robust. The MFOM method, as is evident from Figure B.1 (a-d), becomes more vulnerable as the J/S ratio increases. Of course the average degradation in MSE values, in this jamming scenario, is greater for both methods when compared to the corresponding values in Table 6.5, but this is expected since the jamming conditions are more intense.

B. RESULTS OF JAMMING FOR HP-ADS DATA WITH T_S=185.185 (NSEC)

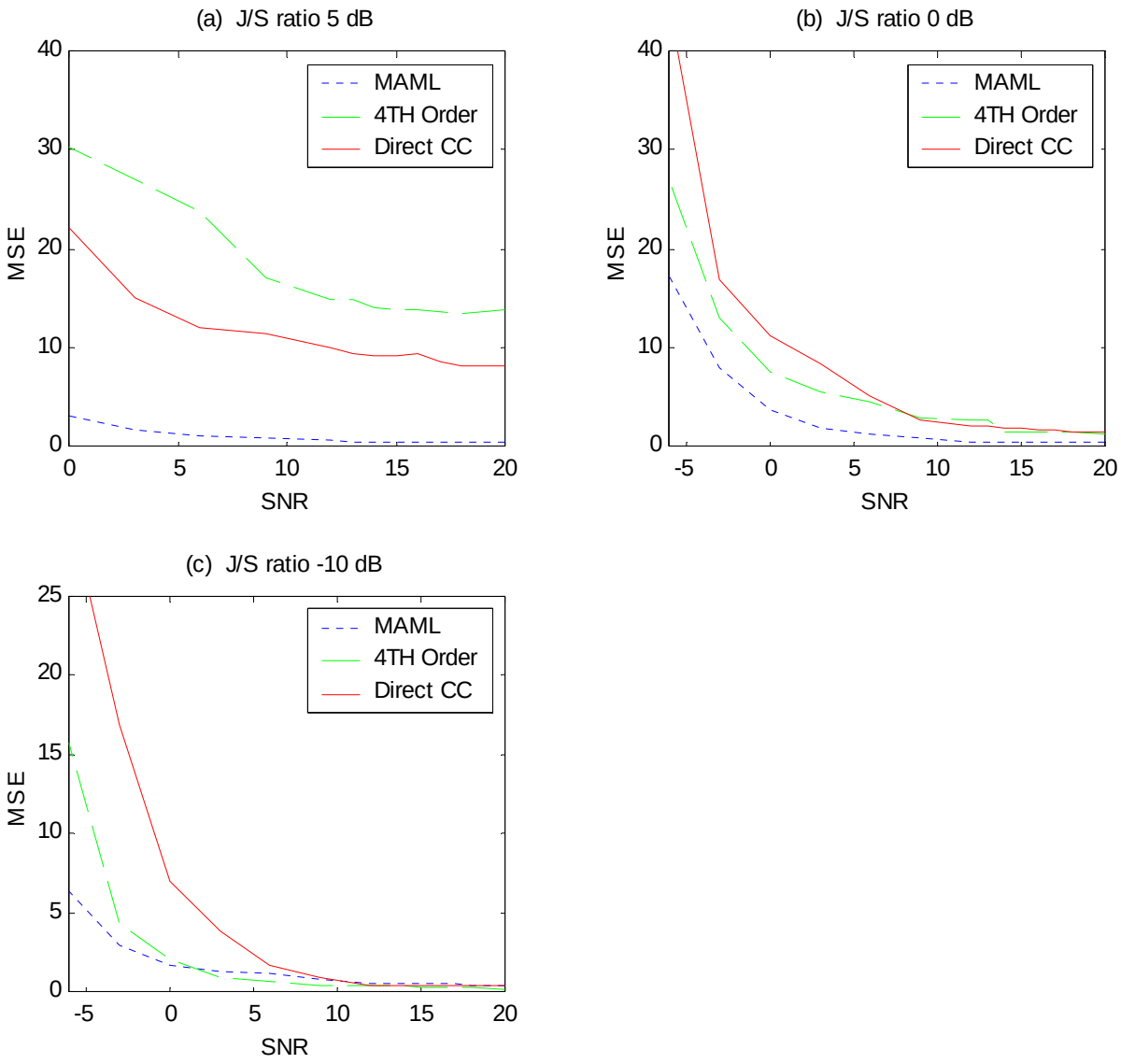

Figure B.2. MSE versus SNR at different jamming-to-signal (J/S) ratios (Data with T_s=185.185 (nsec))

Jamming-to-signal ratio (dB)	**Average Percentage Degradation % for HP-ADS data with sampling Interval 185.185 (nsec)**	
	MAML method	Modified 4^{TH} Order Moment method
10	N/A	N/A
5	82.73	98.94
0	82.62	93.34
-10	67.60	69.78

Table B.2. Average percentage degradation in MSE at various jamming-to-signal ratios (J/S)

C. RESULTS OF JAMMING FOR HP-ADS DATA WITH T_S=92.59 (NSEC)

In this jamming situation the application of the denoising methods did not yield reasonable results. The MSE values obtained were very high and the denoising was not beneficial. Only in the case that the jamming-to-signal (J/S) ratio is below –10 dB, we are able to obtain meaningful MSE values. The plot for –10 dB J/S ratio, can be viewed in the Figure B.3.

Summarizing, we can say that the proposed denoising methods are beneficial even in a severe jamming environment.

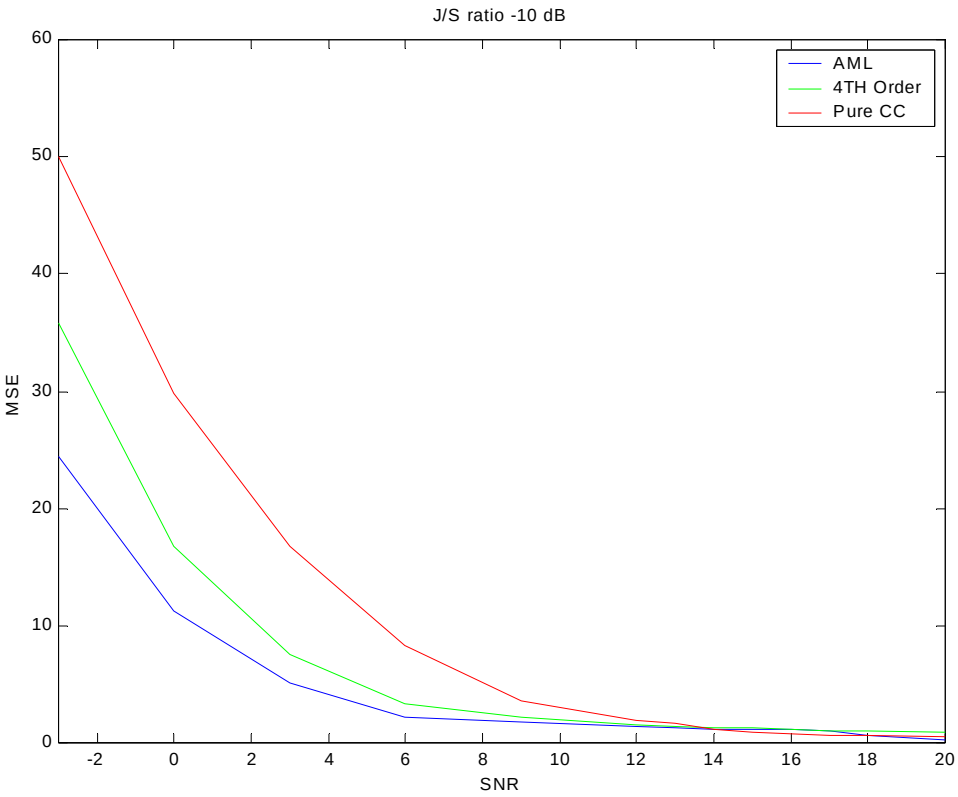

Figure B.3. MSE versus SNR for HP-ADS data with sampling interval T_s=92.59 (nsec), at J/S ratio –10 dB

THIS PAGE INTENTIONALLY LEFT BLANK

APPENDIX C. MATLAB CODES

A. MODIFIED APPROXIMATE MAXIMUM LIKELIHOOD METHOD (MAML)

```
%************************************************************
%************************************************************
% DenoiseMAML: Modified Approximate Maximum Likelihood delay
%              estimation via orthogonal wavelet transform.
%              In this function we perform the wavelet
%              transform of the signal, compute the weights,
%              modify the decomposition coefficients, and
%              recombine the modified coeficients, using the
%              inverse wavelet transform, to obtain the
%              denoised signal.
%
% SYNTAX: y = DenoiseMAML(xn,yn)
%
% INPUT: xn = Received signal from first receiver
%        yn = Received signal from second receiver
%
% OUTPUT:y = Denoised signal
%
%
% SUB_FUNC: None
% Written by Spiros Mantis
%************************************************************
%************************************************************

function y=DenoiseMAML(xn,yn);

xyn=xcorr(xn,yn,'biased');
[sigmas b]=max(xyn);
rx=xcorr(xn,'biased');
maxx=rx(length(xn));
ry=xcorr(yn,'biased');
maxy=ry(length(yn));
sigman1=maxx-sigmas;
sigman2=maxy-sigmas;

nx=wmaxlev(length(xn),'db4');;

[cx lx]=wavedec(xn,nx,'db4');


dxc=[];
for i=1:nx
   d=detcoef(cx,lx,i);
   dl=length(d);
   sigmad=(1/dl)*sum(d.^2);
   sigmasd=sigmad-sigman1;
```

```
   sigmaa(i)=(2^(nx-1))*sigmasd;
   if sigmasd<=0
      wd=0;
   else
      wd=sigmasd/(sigman1*sigman2+sigmasd*(sigman1+sigman2));
   end
   dc=wd*d;
   dxc=[dc dxc];
end

a=appcoef(cx,lx,'db4',nx);
al=length(a);
aux=sum(sigmaa);
sigmasa=((2^nx))*sigmas-aux;
if sigmasa<=0
   wa=0;
else
   wa=sigmasa/(sigman1*sigman2+sigmasa*(sigman1+sigman2));
end
ac=wa*a;
dxc=[ac dxc];

xd=waverec(dxc,lx,'db4');
y=xd;
```

```
%*************************************************
%*************************************************
%
% MAML_main: This is a test program for the Modified
%            Approximate Maximum Likelihood method.
%            In this program we used GSM signals
%            which were generated with the help of
%            the HP-ADS software.
%
% SYNTAX: MAML_main
%
% INPUT: None
%
% OUTPUT: Mean Square Error (MSE) versus SNR
%
% SUB_FUN: DenoiseMAML.m
%
% Written by Spiros Mantis
%*************************************************
%*************************************************

clear all

data_370_set1
s=transpose(s2);
sl=length(s);
pow=(1/sl)*sum(abs(s).^2);


K=100    % number of realizations
rand('seed',40);
f=150*rand(1,K);
delay=floor(f);
delay(1:K/2)=-delay(1:K/2); % delay is between
                            % -150 to +150 samples


n=[20 18 17 16 15 14 13 12 9 6 3 0 -3 -6];
SNR=10.^(n./10);

for k=1:length(SNR)

   oran=SNR(k)
   for i=1:K

      x=[zeros(1,200) s zeros(1,224)];
      y=[zeros(1,200+delay(i)) s zeros(1,224-delay(i))];

      randn('state',2*(i+j));
      noi1_real=sqrt(pow/(2*oran))*randn(1,1024);

      randn('state',3*(i+j));
      noi1_imag=sqrt(pow/(2*oran))*randn(1,1024);

      randn('state',4*(i+j));
      noi2_real=sqrt(pow/(2*oran))*randn(1,1024);
```

```
      randn('state',5*(i+j));
      noi2_imag=sqrt(pow/(2*oran))*randn(1,1024);

      noi1=noi1_real+j*noi1_imag;
      noi2=noi2_real+j*noi2_imag;

      xn=x+noi1; % x + noise
      yn=y+noi2; % y + noise


      % TDOA calculation with xcorr(without denoising)
      xy=xcorr(xn,yn);
      [a1 b1]=max(xy);

      er1(i)=delay(i)-(b1-1024);

      % Denoising using the MAML method
      x_real=DenoiseMAML(real(xn),real(yn));
      y_real=DenoiseMAML(real(yn),real(xn));
      x_imag=DenoiseMAML(imag(xn),imag(yn));
      y_imag=DenoiseMAML(imag(yn),imag(xn));

      X=x_real+j*x_imag;
      Y=y_real+j*y_imag;

      % TDOA calculation with xcorr (with denoising)
      XY=xcorr(X,Y);
      [a2 b2]=max(XY);

      er8(i)=delay(i)-(b2-1024);



   end

   errorMAML(k)=(1/length(er8))*sum(er8.^2);
   error1aMAML(k)=(1/length(er1))*sum(er1.^2);

   Hmaml(k,:)=er8;
   H1amaml(k,:)=er1;



end


figure(1)
k=[20 18 17 16 15 14 13 12 9 6 3 0 -3 -6];
plot(k,error1aMAML(1:14),'o',k,errorMAML(1:14),'x',k,error1aMAML(1:14),
k,errorMAML(1:14))
legend('Direct CC','MAML')
title('Denoise MAML method for HP-ADS data 370.370 (nsec)')
ylabel('MSE')
xlabel('SNR')
figure(2)
plot(1:2047,xy)
title('Correlation Function of x and y signals with noise')
```

```
figure(3)
plot(1:2047,XY)
title('Correlation Function of x and y signals without noise')



save errorMAML;
save error1aMAML;

save Hmaml;
save H1amaml;
```

B. MODIFIED FOURTH ORDER MOMENT METHOD (MFOM)

```
%*********************************************************
%*********************************************************
% DenoiseMFOM: Modified Fourth Order Moment delay estimation
%              via orthogonal wavelet transform.
%              In this function we perform the wavelet
%              transform of the signal, modify the
%              decomposition coefficients by thresholding,
%              and recombine the modified coeficients,
%              using the inverse wavelet transform, to
%              obtain the denoised signal.
%
% SYNTAX: y = DenoiseMFOM(xn,yn)
%
% INPUT: xn = Received signal from first receiver
%        yn = Received signal from second receiver
%
% OUTPUT: y = Denoised signal Xn based on Yn statistics
%
%
% SUB_FUNC: None
% Written by Spiros Mantis
%*********************************************************
%*********************************************************

function y=DenoiseMFOM(xn,yn);

xyn=xcorr(xn,yn,'biased');
[sigmas b]=max(xyn);
rx=xcorr(xn,'biased');
maxx=rx(length(xn));
ry=xcorr(yn,'biased');
maxy=ry(length(yn));
sigman1=maxx-sigmas;
sigman2=maxy-sigmas;

lamdax=3.1*sigman1^2;
nx=wmaxlev(length(xn),'db4');
[cx lx]=wavedec(xn,nx,'db4');

dxc=[];
for i=1:nx
   d=detcoef(cx,lx,i);
   dl=length(d);

   for j=1:dl
      if d(j)^2<1.76*sigman1
         d(j)=0;
      else
         d(j)=d(j);
      end
   end
```

```
A=(1/dl)*sum(d.^4);

   if A<lamdax
     dc=zeros(1,dl);
   else
      dc=d;
   end

   dxc=[dc dxc];
end

a=appcoef(cx,lx,'db4',nx);
al=length(a);
for m=1:al
   if a(m)^2<1.76*sigman1
      a(m)=0;
   else
      a(m)=a(m);
   end
end
A=(1/al)*sum(a.^4);

if A<lamdax
  ac=zeros(1,al);
else
  ac=a;
end

dxc=[ac dxc];

xd=waverec(dxc,lx,'db4');

y=xd;
```

```
%*************************************************
%*************************************************
% MFOM_main: This is a test program for the Modified
%            Fourth Order Moment method.
%            In this program we used GSM signals
%            which were generated with the help of
%            the HP-ADS software.
%
%
% SYNTAX: MFOM_main
%
% INPUT: None
%
% OUTPUT: Mean Square Error (MSE) versus SNR
%
% SUB_FUNC: DenoiseMFOM.m
%
% Written by Spiros Mantis
%*************************************************
%*************************************************

clear all

data_370_set1
s=transpose(s2);
sl=length(s);
pow=(1/sl)*sum(abs(s).^2);


K=100    % number of realizations
rand('seed',40);
f=150*rand(1,K);
delay=floor(f);
delay(1:K/2)=-delay(1:K/2);  % delay is between
                             % -150 to +150


n=[20 18 17 16 15 14 13 12 9 6 3 0 -3 -6];
SNR=10.^(n./10);

for k=1:length(SNR)

   oran=SNR(k)
   for i=1:K

      x=[zeros(1,200) s zeros(1,224)];
      y=[zeros(1,200+delay(i)) s zeros(1,224-delay(i))];

      randn('state',2*(i+j));
      noi1_real=sqrt(pow/(2*oran))*randn(1,1024);

      randn('state',3*(i+j));
      noi1_imag=sqrt(pow/(2*oran))*randn(1,1024);

      randn('state',4*(i+j));
      noi2_real=sqrt(pow/(2*oran))*randn(1,1024);
```

```
      randn('state',5*(i+j));
      noi2_imag=sqrt(pow/(2*oran))*randn(1,1024);

      noi1=noi1_real+j*noi1_imag;
      noi2=noi2_real+j*noi2_imag;

      xn=x+noi1; % x + noise
      yn=y+noi2; % y + noise


      % TDOA calculation with xcorr(without denoising)
      xy=xcorr(xn,yn);
      [a1 b1]=max(real(xy));

      er1(i)=delay(i)-(b1-1024);

      % Denoising using the MFOM method
      X_real=DenoiseMFOM(real(xn),real(yn));
      X_imag=DenoiseMFOM(imag(xn),imag(yn));
      Y_real=DenoiseMFOM(real(yn),real(xn));
      Y_imag=DenoiseMFOM(imag(yn),imag(xn));
      X=X_real+j*X_imag;
      Y=Y_real+j*Y_imag;

      % TDOA calculation with xcorr (with denoising)
      XY=xcorr(X,Y);
      [a2 b2]=max(real(XY));

      er10(i)=delay(i)-(b2-1024);



   end

   errorMFOM(k)=(1/length(er10))*sum(er10.^2);
   error1aMFOM(k)=(1/length(er1))*sum(er1.^2);

   Hmfom(k,:)=er10;
   HMFOM(k,:)=er1;



end


figure(1)
k=[20 18 17 16 15 14 13 12 9 6 3 0 -3 -6];
plot(k,error1aMFOM(1:14),'o',k,errorMFOM(1:14),'x',k,error1aMFOM(1:14),
k,errorMFOM(1:14))
legend('Direct CC','MFOM')
title('Denoise MFOM method for HP-ADS data 370.370 (nsec)')
ylabel('MSE')
xlabel('SNR')
figure(2)
plot(1:2047,xy)
title('Correlation Function of x and y signals with noise')
figure(3)
```

```
plot(1:2047,XY)
title('Correlation Function of x and y signals without noise')



save errorMFOM;
save error1aMFOM;

save Hmfom;
save HMFOM;
```

C. JAMMING

```
%*****************************************************
%*****************************************************
%  Jammer:  Genaration of the noise jamming waveform.
%           This programm generates the "Erfed" FM
%           Noise, used as jamming waveform in our
%           simmulations.
%
%  SYNTAX:  Jammer
%
%  INPUT:   None
%
%  OUTPUT:  1) "Erfed" FM noise jamming waveform
%           2) Power spectrum of the "Erfed" FM noise
%           3) Power spectrum of the HP-ADS signal
%
%  Written by: Spiros Mantis
%
%*****************************************************
%*****************************************************

clear all

%  Load the data generated from the HP-ADS
data_370_set1;
s=transpose(s2);
sl=length(s);
pow=(1/sl)*sum(abs(s).^2);
rand('seed',40)

%  Define the desired SNR
SNR=10^(50/10);
oran=SNR;
y=[zeros(1,200) s zeros(1,224)];

%  Generation of the noisy signal
randn('state',2*(i+j))
noise_real=sqrt(pow/(2*oran))*randn(1,1024);
randn('state',3*(i+j))
noise_imag=sqrt(pow/(2*oran))*randn(1,1024);
noise=noise_real+j*noise_imag;
yn=y+noise;

%  FFT of the noisy signal
S_spect=fft(yn);
S_spect1=S_spect.*conj(S_spect);
S=fftshift(S_spect1);
S1=S/max(S);
figure (1)
plot(10*log10(S1))

%  Define the desired signal-to-jamming ratio
oranj=10^(0/10);
```

```
%  Define Time Vector -tmax to tmax
N=1024;
tmax=1024/(2*(2.7*10^6));
t=2*tmax*(-N/2:N/2-1)/N;

%  Sample Frequency fs
fs=N/(2*tmax);

%  Generate Gaussian Noise Vector
randn('state',6*(i+j))
n=randn(1,N);
figure (2)
subplot(2,2,1);plot(t,n);grid;
xlabel('Time');ylabel('Noise Voltage');
title('Gaussian Noise Voltage');

%  Generate 'Erfed' Noise
yfm=erf(n);

%  Shape Noise with Elliptical Filter
[b,a]=ellip(6,0.5,0.5,0.009);
v=filter(b,a,n);
verf=filter(b,a,yfm);

%  Define VCO with k=300 KHz/v
f0=0;k=300000;
f=f0+k*v;
f1=f0+k*verf;
x=sqrt(pow/(2*oranj))*cos(2*pi*f.*t)+j*sqrt(pow/(2*oranj))*sin(2*pi*f.*
t);
xerf=sqrt(pow/(oranj))*cos(2*pi*f1.*t)+sqrt(pow/(oranj))*sin(2*pi*f1.*t
);

%  Find Power Spectrum for v(t)
V=fft(v);
Pv=V.*conj(V);
Pv=fftshift(Pv);

%  Find Power Spectrum for x(t) and xerf(t)
X=fft(x);
XE=fft(xerf);
Px=X.*conj(X);
Pxe=XE.*conj(XE);
Px=fftshift(Px);
Pxe=fftshift(Pxe);


%  Normalize Amplitude
Px1=Px/max(Px);Pv1=Pv/max(Pv);Pxe1=Pxe/max(Pxe);
Pxdbm=10*log10(Px1);
Pvdbm=10*log10(Pv1);
Pxedbm=10*log10(Pxe1);

%  Select frequency axis
fsam=fs*(-1024/2:1024/2-1)/1024;
```

```
%  Plot control noise spectrum
subplot(2,2,2);
plot(fsam,Pvdbm);grid;
xlabel('Hz');ylabel('DBM');
title('Noise Spectrum');

%  Plot 'Erfed' FM noise spectrum
subplot(2,2,3);
plot(fsam,Pxedbm,'r');grid;
axis([-1.2*10^6,1.2*10^6,-50,30]);
xlabel('Hz')
ylabel('DB');
title('Erfed FM Noise Spectrum');

%  Plot Erfed FM noise waveform
subplot(2,2,4);
plot(1:1024,real(xerf))
xlabel('Samples');
title('Jamming waveform');grid

%  Generation of the NOISE+Jamming+SIGNAL
yn1=y+noise+xerf;

%  FFT of the SIGNAL+NOISE+JAMMING
S_spectjam=fft(yn1);
S_spect1jam=S_spectjam.*conj(S_spectjam);
Sjam=fftshift(S_spect1jam);
S1jam=Sjam/max(Sjam);

figure (3)
subplot(3,1,2)
plot(1:1024,real(xerf))
title('Erfed waveform')
subplot(3,1,1)
plot(1:1024,real(yn))
title('Noisy signal')
subplot(3,1,3)
plot(1:1024,real(yn1))
title('Signal + Noise + Jamming')
```

```
%*************************************************************
%*************************************************************
%
% Jamming_main: This is a test program the MAML method or the
%               MFOM method, when jamming is present.
%               In this program, we used the HP-ADS GSM signals.
%               We also used the "Erfed" FM noise jamming
%               waveform, which is added only in one channel.
%
% SYNTAX: Jamming_main
%
% INPUT: None
%
% OUTPUT: Mean Square Error (MSE) versus SNR
%
% SUB_FUN: DenoiseMAML.m
%          DenoiseMFOM.m
%
% Written by Spiros Mantis
%*************************************************************
%*************************************************************

clear all

data_370_set1
s=transpose(s2);
sl=length(s);
pow=(1/sl)*sum(abs(s).^2);

K=100    % number of realizations
rand('seed',40);
f=150*rand(1,K);
delay=floor(f);
delay(1:K/2)=-delay(1:K/2);  % delay is between
                             % -150 to +150


%  Define the desired signal-to-jamming ratios
Jammer=[-10 -5 0 10];

     for m=1:4

          n=[20 18 17 16 15 14 13 12 9 6 3 0 -3 -6];
          SNR=10.^(n./10);
          oranj=10^(Jammer(m)/10);
          %  Define Time Vector -tmax to tmax
          N=1024;
          tmax=N/(2*(10.8*10^6));
          t=2*tmax*(-N/2:N/2-1)/N;
          %  Sample Frequency fs
          fs=N/(2*tmax);
          %  Generate Gaussian Noise Vector
          randn('state',6*(i+j));
          noi=randn(1,1024);
          %  Generate 'Erfed' Noise
          yfm=erf(noi);
          %  Shape Noise with Elliptical Filter
```

```
          [bfm,afm]=ellip(6,0.5,0.5,0.04);
          v=filter(bfm,afm,noi);
          verf=filter(bfm,afm,yfm);
          %  Define VCO with k=500 KHz/v
          f0=0;kfm=500000;
          fm=f0+kfm*v;
          f1=f0+kfm*verf;

xfm=sqrt(pow/(2*oranj))*cos(2*pi*fm.*t)+j*sqrt(pow/(2*oranj))*sin(2*pi*
fm.*t);

xerf=sqrt(pow/(oranj))*cos(2*pi*f1.*t)+sqrt(pow/(oranj))*sin(2*pi*f1.*t
);

               for k=1:length(SNR)

                    oran=SNR(k);
                    n(k)
                    Jammer(m)
                         for i=1:K

                              x=[zeros(1,200) s zeros(1,224)];
                              y=[zeros(1,200+delay(i)) s zeros(1,224-
                                 delay(i))];
                              randn('state',2*(i+j));
                             noi1_real=sqrt(pow/(2*oran))*randn(1,1024);
                              randn('state',3*(i+j));
                             noi1_imag=sqrt(pow/(2*oran))*randn(1,1024);
                              randn('state',4*(i+j));
                             noi2_real=sqrt(pow/(2*oran))*randn(1,1024);
                              randn('state',5*(i+j));
                             noi2_imag=sqrt(pow/(2*oran))*randn(1,1024);
                              noi1=noi1_real+j*noi1_imag;
                              noi2=noi2_real+j*noi2_imag;
                              xn=x+noi1+xerf; % x + noise
                              yn=y+noi2; % y + noise
                              % TDOA calculation with xcorr( without
                                denoising)
                              xy=xcorr(xn,yn);
                              [a1 b1]=max(real(xy));
                              er1(i)=delay(i)-(b1-1024);
                              % Denoise using MAML method
                              x_real=DenoiseMAML(real(xn),real(yn));
                              y_real=DenoiseMAML(real(yn),real(xn));
                              x_imag=DenoiseMAML(imag(xn),imag(yn));
                              y_imag=DenoiseMAML(imag(yn),imag(xn));
                              X=x_real+j*x_imag;
                              Y=y_real+j*y_imag;
                              % TDOA calculation with xcorr(with
                                denoising)
                              XY=xcorr(X,Y);
                              [a2 b2]=max(real(XY));
                              er8(i)=delay(i)-(b2-1024);


                         end
```

```
                    error8JAM(k)=(1/length(er8))*sum(er8.^2);
                    error1aJAM(k)=(1/length(er1))*sum(er1.^2);
                    H8JAM(k,:)=er8;
                    H1aJAM(k,:)=er1;
               end

          figure(m)
          k=[20 18 17 16 15 14 13 12 9 6 3 0 -3 -6];

plot(k,error1aJAM(1:14),'o',k,error8JAM(1:14),'x',k,error1aJAM(1:14),k,
error8JAM(1:14))
          legend('Direct CC','MAML')
          title('MAML method with Jamming for HP-ADS data 370.370
                (nsec)')
          ylabel('MSE')
          xlabel('SNR')

          ERROR8JAM(m,:)=error8JAM;
          ERROR1aJAM(m,:)=error1aJAM;

     end

figure (5)
plot(k,ERROR8JAM(1,:),'r',k,ERROR8JAM(2,:),'b',k,ERROR8JAM(3,:),'g',k,E
RROR8JAM(4,:),'c')
legend('-10dB S/J ratio','-5dB S/J ratio','0dB S/J ratio','10dB S/J
       ratio')
title('MAML method with Jamming for HP-ADS data 370.370 (nsec)')
xlabel('SNR')
ylabel('MSE')
```

LIST OF REFERENCES

1. FCC Report and Order and Further Notice of Proposed Rule Making, FCC, Docket 96-264, June 1996.

2. http://www.fcc.cov/e911

3. FCC Third Report and Order, FCC, Docket 99-245, September 15, 1999.

4. http://www.comm-nav.com/e911.htm

5. Conference of European Posts and Telecommunications, http://www.eto.dk/ceptectra/ceptinfo.htm

6. GSM Association, http://www.gsmworld.com/statistics/.

7. Rappaport, T. S., *Wireless Communications: Principles & Practice*, Upper Saddle River, NJ, Prentice Hall, 1997.

8. Garg, V. K., and Wilkens, J. E., *Principles & Applications of GSM*, Upper Saddle River, NJ Prentice Hall, 1999.

9. Mehrota, A., *GSM System Engineering*, Norwood, MA, Artech House Publishers, 1997.

10. Saucier and Strucman, "Direction finding using correlation techniques," *Proceeding of IEEE International Symposium on Antennas and Propagation*, Pg. 260-263, June 1975.

11. Knorr, J., "Shipboard HFDF System Simulation," ACES Journal, pg. 25-42, March 1998.

12. Kennedy, J., and Sullivan, M. C., "Direction Finding and Smart Antennas Using Software Radio Architecture," IEEE Communications Magazine, vol. 33, no. 5, May 1995, pg. 62-68.

13. Rappaport, T. S., Reed, J. H., and Woerner, B. D., "Position Location Using Wireless Communications on Highways of the Future," IEEE Communications Magazine, October 1996, pg. 33-41.

14. Krizman, K. J., Biedka, T. E., and Rappaport, T. S., "Wireless Position Location: Fundamentals, Implementation Strategies, and Sources of Error," *IEEE Transactions on Communications*, March 1997, pg. 919-923.

15. Chan, Y. T., and Ho, K. C., "A Simple and Efficient Estimator for Hyperbolic Location," *IEEE Transactions on Signal Processing*, vol. 42, no. 8, August 1994 Pg. 1905-1915.

16. Smith, O. J., and Abel, J. S., "The Spherical Interpolation Method of Source Localization," IEEE Journal in Oceanic Engineering, vol. OE-12, no. 1, January 1987, pg. 246-252.

17. Foy, W. H., "Position Location Solutions by Taylor Series Estimation," *IEEE Transactions on Aerospace and Electronic Systems*, vol. AES-12, no. 2, March 1976, pg. 187-193.

18. Chan, Y. T., So, H. C., and Ching, P. C., "Approximate Maximum Likelihood Delay Estimation via Orthogonal Wavelet Transform," *IEEE Transactions on Signal Processing*, vol. 47, no. 4, April 1999, pg. 1193-1198.

19. Aktas, U., *Time Difference of Arrival (TDOA) Estimation Using Wavelet Based Denoising*, Master's Thesis, Naval Postgraduate School, Monterey, CA, March 1999.

20. Hippenstiel, R, and Mantis, S., "Wavelet Denoising of Signals Based on the Fourth Order Moment Method," accepted for presentation at the *6th International Symposium on Signal Processing and its Applications (ISSPA)*, August 2001.

21. Software Hewelett-Packard, Advanced Design System (HP-ADS), version 1.1, Hewlett-Packard Company, Palo Alto, CA, 1998.

22. Haney, T., *Generation of Global System for Mobile (GSM) Signals and their Time Difference of Arrival (RDOA) Estimation*, Master's Thesis, Naval Postgraduate School, Monterey, CA, June 2000.

23. Schleher, C. D., *Electronic Warfare in the Information Age*, Artech House Inc., Norwood, MA, 1999.

24. Boyd, J.A., *Electronic Countermeasures*, Peninsula Publishing, Los Altos, CA, 1965.

25. The Matlab software version 5.3, The Mathworks Inc., Natick, MA, 1999.

26. Burrus, C. S., Gopinath, R. A., and Guo, H., *Introduction to Wavelet Transforms*, Prentice Hall, Upper Saddle River, NJ, 1998.

27. Strang, G., and Nquyen, T., *Wavelets and Filter Banks*, Welleseley-Cambridge Press, Wellesley, MA, 1996.

28. Mantis, S., and Hippenstiel, R., “Time Difference of Arrival Estimation of Unequal SNR Denoised Communication Signals,” *Proceedings of 34th Asilomar Conference on Signals, Systems and Computers*, Volume 1, October 2000.

THIS PAGE INTENTIONALLY LEFT BLANK

INITIAL DISTRIBUTION LIST

1. Defense Technical Information Center 2
   8725 John J. Kingman Road, Suite 0944
   Ft. Belvoir, VA 22060-6218

2. Dudley Knox Library 2
   Naval Postgraduate School
   411 Dyer Road
   Monterey, CA 93943-5101

3. Engineering and Technology Curricular Office 1
   Code 34
   Naval Postgraduate School
   Monterey, CA, 93943-5107

4. Information Warfare Curricular Office 1
   Code 37
   Naval Postgraduate School
   Monterey, CA, 93943-5140

5. Chairman, Code EC 1
   Department of Electrical and Computer Engineering
   Naval Postgraduate School
   Monterey, CA, 93943-5121

6. Professor Dan Boger, Code IW/Bd 1
   Chairman, IW Academic Group
   Naval Postgraduate School
   Monterey, CA, 93943-5140

7. Professor Ralph D. Hippenstiel, Code EC/Hi 2
   Department of Electrical and Computer Engineering
   Naval Postgraduate School
   Monterey, CA, 93943-5121

8. Professor David C. Jenn, Code EC/Jn 1
   Department of Electrical and Computer Engineering
   Naval Postgraduate School
   Monterey, CA, 93943-5121

9. Professor Tri T. Ha, Code EC/Ha 1
Department of Electrical and Computer Engineering
Naval Postgraduate School
Monterey, CA, 93943-5121

10. Embassy of Greece..... 1
Naval Attache Office
2228 Massachusetts Avenue, N.W.
Washington, DC, 20008

11. Spiros Mantis..... 2
Ermou 8, Agios Nikolaos
Salamina, TK 18900
GREECE-HELLAS